

Stochastic Geometry Analysis of IRS-Assisted Downlink Cellular Networks

Taniya Shafique, Hina Tabassum, and Ekram Hossain

Abstract

Using stochastic geometry tools, we develop a comprehensive framework to analyze the downlink coverage probability, ergodic capacity, and energy efficiency (EE) of various types of users (e.g., users served by direct base station (BS) transmissions and indirect intelligent reflecting surface (IRS)-assisted transmissions) in a cellular network with multiple BSs and IRSs. The proposed stochastic geometry framework can capture the impact of channel fading, locations of BSs and IRSs, arbitrary phase-shifts and interference experienced by a typical user supported by direct transmission and/or IRS-assisted transmission. For IRS-assisted transmissions, we first model the desired signal power from the nearest IRS as a sum of scaled generalized gamma (GG) random variables whose parameters are functions of the IRS phase shifts. Then, we derive the Laplace Transform (LT) of the received signal power in a closed form. Also, we model the aggregate interference from multiple IRSs as the sum of normal random variables. Then, we derive the LT of the aggregate interference from all IRSs and BSs. The derived LT expressions are used to calculate coverage probability, ergodic capacity, and EE for users served by direct BS transmissions as well as users served by IRS-assisted transmissions. Finally, we derive the overall network coverage probability, ergodic capacity, and EE based on the fraction of direct and IRS-assisted users, which is defined as a function of the deployment intensity of IRSs, as well as blockage probability of direct transmission links. Numerical results validate the derived analytical expressions and extract useful insights related to the number of IRS elements, large-scale deployment of IRSs and BSs, and the impact of IRS interference on direct transmissions.

Index Terms

Intelligent reflecting surfaces, phase-shifts, stochastic geometry, interference, ergodic capacity, coverage probability, energy-efficiency, Laplace transform.

T. Shafique and E. Hossain are with the Department of Electrical and Computer Engineering, University of Manitoba, Canada.
H. Tabassum is with the Department of Electrical Engineering and Computer Science, York University, Canada.

I. INTRODUCTION

Intelligent reflecting surfaces (IRSs) are considered as a key enabling technology for the sixth generation (6G) wireless communications systems. IRSs enable a smart manipulation of the wireless propagation environment [1], [2]. Each IRS consists of many antenna elements (a.k.a. IRS elements) [3] and each IRS element is controlled via a controller that assists each IRS element to steer the incident signal into the desired direction [4]. Also, with the advances in the wireless technology and extravagant demand of higher data rate to millions of indoor/outdoor devices, it has become inevitable to utilize the resources wisely to enable massive connectivity. In this context, IRSs operate as a low cost solution to extend the communication range and to provide service to more users. In order to achieve this goal, the transmissions can happen in three modes, i.e., (i) *Joint Transmission*: in which a user receives the IRS signals combined with the direct signal from the base-stations (BSs), (ii) *IRS-only Transmission*: in which a user receives only IRS transmissions and the direct transmissions get blocked, and (iii) *Direct Transmission*: in which a user gets served only through direct transmissions.

It is noteworthy that combining the signals coming from the direct and indirect IRS-assisted path may suffer from incoherent multi-path delays and it may necessitate sophisticated synchronization, detection, and co-phasing techniques resulting in complex hardware/software design. Furthermore, the impact of IRS transmissions is generally more understandable in the absence of direct link; therefore, it is crucial to investigate the significance of IRS-only transmissions without direct links. Similarly, the fact that the direct transmissions from BSs may be impacted by the presence of IRSs, it is important to study the performance of direct transmissions in a large-scale IRS-assisted network comprehensively. In this paper, we develop a novel framework to analyze the performance of various types of transmissions in a multi-BS, multi-IRS network.

A. Background Work

To date, there have been a number of research works that considered the performance analysis of IRS-assisted communication systems assuming a single IRS, single source and destination [5]–[12]. For instance, the authors in [5] applied the central limit theorem (CLT) to derive the approximate symbol error probability expressions under independent Rayleigh fading channels. In [6], the authors derived the approximate outage probability, symbol error rate, and upper and lower bounds on ergodic capacity by applying CLT and assuming uncorrelated Rayleigh fading channels. Later, [7] derived the average bit error rate, capacity, and outage probability with

Rayleigh fading. In [8], the exact outage probability, symbol error rate, and ergodic capacity expressions under Rayleigh fading were derived. In [9] and [10], using moment generating function (MGF)-based approach, the exact outage probability was derived considering *Nakagami- m* and generalized fading channels, respectively. The direct link transmission was ignored in [5]–[7], [9]; however [10] considered both the direct and IRS-assisted transmissions. In [11], the authors derived the outage probability and ergodic capacity expressions considering IRS link modeled with Rician fading and direct channel modeled as Rayleigh fading. The joint direct and IRS-assisted transmission was considered.

All of the aforementioned research works were limited to single IRS, single source, and single destination under varying fading channels. That is, the impact of interference is ignored and the IRS is deployed at a fixed location. Furthermore, the analyses assume optimal phase-shifts and apply CLT, which simplifies the cascaded signal model substantially. Recently, in [12], using moment matching method, the authors derived the outage probability and capacity expressions under correlated Rayleigh fading channel while considering arbitrary phase shifts. This work considered both the direct and IRS-assisted links; however, again the framework was limited to a single IRS, single source, and single destination. Another work is [13] where multi-pair D2D network is considered with a single IRS and the authors derive average achievable rate expressions assuming arbitrary phase-shifts. However, the authors considered approximating the signal and interference power with their respective statistical averages.

Another series of research works considered multiple IRSs, single source, and single destination [14]–[16]. In [14], the authors derived the outage probability considering Rayleigh fading with the direct transmission blocked. The transmission is conducted by only one IRS that provides the maximum SNR. Instead of applying CLT, the authors proposed Generalized- K approximation. In [15], the authors applied CLT to derive the outage probability and rate considering Nakagami- m fading. Both the direct and indirect transmissions were considered. Similarly, in [16], the authors derived the outage probability by approximating the end-to-end IRS-assisted channel with the log-normal and gamma distribution.

The aforementioned research works ignored interference from IRSs, assumed a single BS, and ideal phase shifts were assumed. Recently, a couple of research works considered a realistic multi-IRS set-up with multiple BSs [17]. In [17], the authors derived the average achievable rate of the IRS-assisted multi-BS network and derived the Laplace Transform (LT) of the aggregate interference from all BSs and IRSs. However, the interference from all BSs

to a specific IRS is replaced by its average value. The resulting rate expressions require four-fold integral evaluations. Another relevant research work is [18] where the authors derived the coverage probability expressions considering joint direct and IRS transmission. The signal power is approximated with the Gamma distribution and approximated the interference from all IRS with the mean IRS interference. Both of the aforementioned works [17], [18] assumed optimal phase-shifts in the desired signal and interference which makes the application of CLT possible.

B. Paper Contribution and Organization

In this paper, we develop a comprehensive framework to analyze the coverage probability and rate of various types of users (e.g., users performing direct transmissions and indirect IRS-assisted transmissions) in a realistic large-scale multi-BS, multi-IRS network. The proposed framework can capture the impact of arbitrary phase-shifts on the received signal power as well as the aggregate interference from all IRSs on users that are served by direct transmissions from BS or IRS-assisted transmissions. More specifically, we have the following main contributions:

- For IRS-assisted downlink transmissions, we characterize the desired signal power from the nearest IRS as a sum of scaled generalized gamma (GG) random variables whose parameters are a function of the IRS phase shifts. Then, we derive the novel LT expression and validate its accuracy considering both the optimized and randomized phase-shifts of the IRS.
- We characterize the aggregate interference from multiple IRSs in a multiple BS scenario as the sum of normal random variables. Then, we derive the LT of the aggregate interference from all IRSs. The derived expressions can be customized for both types of users, i.e., those served by direct BS transmissions and those served by IRS-assisted transmissions.
- Based on the LT expressions, we characterize the coverage probability, ergodic capacity, and energy-efficiency of both the IRS-assisted users and direct users.
- Finally, we derive the overall coverage probability, ergodic capacity, and energy efficiency based on the fraction of direct and indirect IRS-assisted users in the network. This fraction is derived as a function of the **(i)** deployment intensity of IRSs as well as **(ii)** blockage probability of direct transmission links.
- The analytical results are validated by Monte-Carlo simulations. Numerical results extract useful insights related to the impact of IRS interference on IRS-assisted as well as direct transmissions in a large-scale network as a function of the number of IRS elements, intensity of IRSs and BSs, and the transmit power of BSs.

The remainder of the paper is organized as follows. Section II describes the system model and assumptions and the methodology of analysis. We characterize the statistics of the received signal power, aggregate interference and the corresponding LT of users supported by IRS in Section III and Section IV, respectively. The coverage probability, ergodic capacity and energy efficiency of users supported by IRS transmissions and users supported by direct transmission, also the overall coverage of the network and achievable data rate is provided in Section V. Then, in Section VI, we present selected numerical results followed by conclusions in Section VII. A list of the major notations is presented in **Table 1**.

II. SYSTEM MODEL AND ASSUMPTIONS

In this section, we present the network, transmission, signal and interference models for users who are served by direct BS transmissions and those served by IRS-assisted transmissions, and also our methodology for large-scale analysis of the system.

A. Network Deployment and Transmission Model

We consider a two-tier downlink cellular network consisting of IRS surfaces, BSs, and users within a coverage area of radius R . The locations of the BSs follow a homogeneous Poisson Point Process (PPP) denoted as Φ_B with intensity λ_B , whereas the locations of the IRSs follow Binomial Point Process (BPP) in which M IRSs are distributed uniformly in the coverage region. For simplicity, we refer to $\lambda_R = \frac{M}{\pi R^2}$ as the IRS intensity throughout the paper. We assume that the IRSs are deployed at a fixed height H_R and are equipped with N elements each, whereas all the BSs have a fixed height H_B . We assume that there are two different types of users in the considered multi-BS and multi-IRS network, i.e.,

- *Direct users*: who are served by direct BS transmissions, and
- *IRS-assisted users*: who are served by indirect IRS-assisted transmissions.

The typical user who is deployed at origin would reflect the performance of any user within the coverage region. We also consider \mathcal{A} IRS-assisted users and $1 - \mathcal{A}$ direct users in the system. For direct transmission from the BS, the typical user is associated to the nearest BS. In the indirect IRS-assisted transmission mode, the user associates to the nearest IRS, and then, that nearest IRS associates to the nearest BS (as illustrated in Fig. 1).

We assume that an IRS can relay information from only one BS to only one user at a predefined time/frequency resource to maintain orthogonality. We consider that the *direct* communication

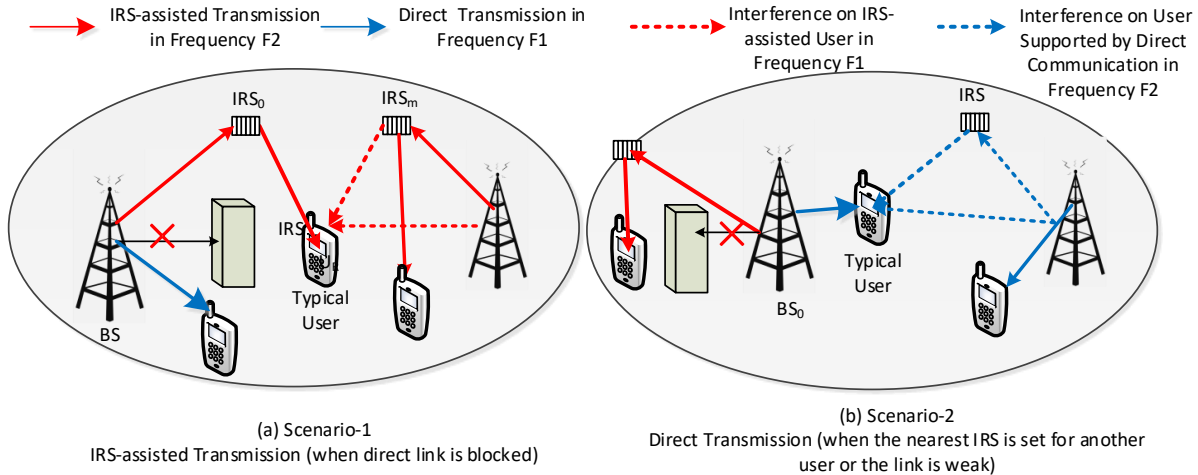


Fig. 1. System model for direct and IRS-assisted communication in multi-IRS and multi-BS setup: (a) Scenario 1: when the user is connected with a BS through nearest IRS and the direct link to the nearest BS is blocked, and (b) Scenario 2: when the user is connected with a nearest BS in the presence a weak IRS link.

(i.e., BS to the typical user) and *indirect* IRS-assisted communication (i.e., BS to IRS and IRS to the typical user) share different frequency spectrum such that a BS can serve both the direct and indirect IRS-assisted users.

B. Signal and Interference Models (IRS-Assisted Users)

1) *Desired Signal Power*: The signal power received at the typical user from the nearest IRS (IRS₀) is given as [13], [19]:

$$S_{R_0} = P |\hat{\mathbf{g}}_{0,0}^H \Theta_0 \hat{\mathbf{f}}_{0,j}|^2 = P \left| \sum_{n=1}^N C_{0n,j} f_{0n,j} g_{0,0n} e^{j\theta_{0n}} \right|^2, \quad (1)$$

where P is the transmission power of the BSs in IRS-assisted mode, $g_{0,0n} = |g_{0,0n}| e^{-j\phi_{0,0n}}$ is the Rayleigh fading channel gain from the typical user to the n -th element of IRS₀, thus $\hat{g}_{0,0n} = \beta (r_{0,0n})^{-\alpha/2} g_{0,0n}$, where $\alpha \geq 2$ represents the path-loss exponent, $\beta = \left(\frac{4\pi f_c}{c}\right)^{-2}$ is the channel power gain on free-space path-loss model at a reference distance of one meter, f_c is carrier frequency, and c represents the speed of light, and $\hat{\mathbf{g}}_{0,0} \in \mathbb{C}^{1 \times N}$, where $r_{0,0n} = \sqrt{\ell_{0n}^2 + H_R^2}$ represents the distance from the n -th element of the IRS₀ to the typical user. Note that $|g_{0,0n}|$ and $\phi_{0,0n}$ represent the magnitude and phase component of the fading channel from the n -th element of IRS₀ to the typical receiver. Similarly, $f_{0n,j} = |f_{0n,j}| e^{-j\psi_{0n,j}}$ is the fading channel

TABLE I
MATHEMATICAL NOTATIONS

Notation	Description	Notation	Description
R	Coverage radius	N	Number of IRS elements
M	Total number of IRSs	λ_B	BS intensity
Φ_B	PPP for BSs	H_B, H_R	BS height, IRS height
α	Path-loss exponent	BS_j	j -th interfering BS to the typical user in direct mode
BS_0	Nearest BS to the typical user in direct mode	ℓ_j	Direct distance of BS_j in 2D
d_j	Direct distance of BS_j in 3D	ℓ_0	Direct distance of nearest BS_0 in 2D
d_0	Direct distance of BS_j in 3D	h_j	Fading channel between typical user and BS_j
h_0	Fading channel between typical user and BS_0	\hat{P}, P	Transmission power of BSs in direct and IRS-assisted mode
IRS_{m_n}	The n -th element of interfering IRS m	IRS_{0_n}	The n -th element of nearest IRS_0 to user
$ g_{0,m_n} , \phi_{0,m_n}$	Fading magnitude and phase from the user to the IRS_{m_n}	r_{0,m_n}	Distance of the user to the IRS_{m_n}
$ f_{m_n,j} , \psi_{m_n,j}$	Fading magnitude and phase from IRS_{m_n} to BS_j	$t_{m_n,j}$	Distance from IRS_{m_n} to BS_j
Θ_{m_n}	Phase shift of IRS_{m_n}	Θ_{0_n}	Phase shift of IRS_{0_n}
$ g_{0,0_n} , \phi_{0,0_n}$	Fading magnitude and phase from the user to the IRS_{0_n}	$r_{0,0_n}$	Distance of the user to the IRS_{0_n}
$ f_{0_n,j} , \psi_{0_n,j}$	Fading magnitude and phase from IRS_{0_n} to BS_j	$t_{0_n,j}$	Distance from IRS_{0_n} to BS_j
I_B	Aggregate interference from all BSs in IRS-assisted mode	I_R	Aggregate interference from all IRS in IRS-assisted mode
\hat{I}_B	Aggregate interference from all BSs in direct mode	\hat{I}_R	Aggregate interference from all IRS in direct mode
S_{D_0}	Received signal power from BS_0	S_{R_0}	Received signal power from IRS_0
C_D	Coverage probability in the direct transmission mode	C_{ID}	Coverage probability in the IRS-assisted mode
γ_D	Direct mode SINR	γ_{ID}	Direct mode SINR
τ	SINR threshold	\mathcal{A}	Fraction of users assisted by IRS
$X_G(\kappa, \zeta)$	Gamma RV and parameters	$X_{GG}(a, d, p)$	Generalized gamma RV and parameters
R_D	Rate achieved in direct mode	R_{ID}	Rate achieved in indirect mode
t_j	Approximation of $t_{m,j}$	N_0	Noise power spectral density
p_{BS}, p_U	Static power consumption of BS and user	p_{IRS}	IRS power consumption
p_{ID}	Total system power consumption per user in ID mode	p_D	Total system power consumption per user in direct mode
\mathcal{A}	Fraction of user associated with IRS-assisted ID communication	β	Reference channel power gain on free space path loss at 1-meter distance

gain from the n -th element of IRS_0 to j -th BS, thus $\hat{f}_{0_n,j} = \beta (t_{0_n,j})^{-\alpha/2} f_{0_n,j}$ and $\hat{\mathbf{f}}_{0,j} \in \mathbb{C}^{N \times 1}$, where

$$t_{0_n,j} = \sqrt{r_{0,0_n}^2 + d_j^2 - 2r_{0,0_n}d_j \cos(\angle t_{0_n,j})}$$

represents the distance from the n -th element of IRS_0 to the typical user, where $\angle t_{0_n,j}$ denotes the angle opposite to $t_{0_n,j}$. Note that $|f_{0_n,j}|$ and $\psi_{0_n,j}$ represent the magnitude and phase component of the fading channel from j -th BS to n -th element of IRS_0 . Finally, Θ_0 denotes the phase shift of the IRS_0 and $\Theta_0 = \text{diag}\{e^{j\theta_{0_1}}, e^{j\theta_{0_2}}, \dots, e^{j\theta_{0_N}}\}$, and $C_{0_n,j} = (r_{0,0_n}t_{0_n,j})^{-\alpha/2}$.

2) *Interference Power*: The interference at a typical user in the IRS-assisted mode is composed of two parts (i) interference from the BSs, and (ii) interference from the IRSs. The aggregate

interference from all the BSs (excluding the nearest BS) is given as follows:

$$I_B = \sum_{j \in \Phi_B \setminus 0} P \beta^2 |h_j|^2 d_j^{-\alpha} = \sum_{j \in \Phi_B \setminus 0} P \beta^2 |h_j|^2 (\ell_j^2 + H_B^2)^{-\alpha/2}, \quad (2)$$

On the other hand, the aggregate interference from the IRSs can be modeled as follows:

$$I_R = \sum_{j \in \Phi_B} \sum_{m=1}^{M \setminus 0} P |\hat{\mathbf{g}}_{0,m}^H \Theta_m \hat{\mathbf{f}}_{m,j}|^2 = \sum_{j \in \Phi_B} \sum_{m=1}^{M \setminus 0} P \left| \sum_{n=1}^N C_{m_n,j} f_{m_n,j} g_{0,m_n} e^{j\theta_{m_n}} \right|^2, \quad (3)$$

where $g_{0,m_n} = |g_{0,m_n}| e^{-j\phi_{0,m_n}}$ is the fading channel gain from the typical user to the n -th element of IRS m , thus $\hat{g}_{0,m_n} = \beta (r_{0,m_n})^{-\alpha/2} g_{0,m_n}$ and $\hat{\mathbf{g}}_{0,m} \in \mathbb{C}^{1 \times N}$, where $r_{0,m_n} = \sqrt{\ell_{m_n}^2 + H_R^2}$ represents the distance from n -th element of m -th IRS to the typical user. Note that $|g_{0,m_n}|$ and ϕ_{0,m_n} represent the magnitude and phase component of the fading channel from n -th element of m -th IRS to the typical receiver. Similarly, $f_{m_n,j} = |f_{m_n,j}| e^{-j\psi_{m_n,j}}$ is the fading channel gain from the n -th element of IRS m to j -th BS, thus $\hat{f}_{m_n,j} = \beta (t_{m_n,j})^{-\alpha/2} f_{m_n,j}$ and $\hat{\mathbf{f}}_{m,j} \in \mathbb{C}^{N \times 1}$, where $t_{m_n,j} = \sqrt{r_{0,m_n}^2 + d_j^2 - 2r_{0,m_n} d_j \cos(\angle t_{m_n,j})}$ represents the distance from n -th element of m -th IRS to the typical user where $\angle t_{m_n,j}$ denotes the angle opposite to $t_{m_n,j}$. Note that $|f_{m_n,j}|$ and $\psi_{m_n,j}$ represent the magnitude and phase component of the fading channel from j -th BS to n -th element of m -th IRS. Finally, Θ_m denotes the phase shift of the IRS and $\Theta_m = \text{diag}\{e^{j\theta_{m_1}}, e^{j\theta_{m_2}}, \dots, e^{j\theta_{m_N}}\}$, and $C_{m_n,j} = (r_{0,m_n} t_{m_n,j})^{-\alpha/2}$.

C. Signal and Interference Models (Direct Mode)

1) *Desired Signal Power*: The signal power from the desired BS to the typical user is:

$$S_{D_0} = \hat{P} \beta^2 |h_0|^2 d_0^{-\alpha} = \hat{P} \beta^2 |h_0|^2 (\ell_0^2 + H_B^2)^{-\alpha/2}, \quad (4)$$

where \hat{P} is the transmission power of the BSs in direct mode, h_0 and d_0 are the small scale fading channel and the distance between the typical user to the nearest BS, respectively.

2) *Interference Power*: The interference at a typical user in the direct mode is composed of two parts (i) interference from the BSs, and (ii) interference from the IRSs. The aggregate interference from the BSs (excluding the desired BS) is given as follows:

$$\hat{I}_B = \sum_{j \in \Phi_B \setminus 0} \hat{P} \beta^2 |h_j|^2 d_j^{-\alpha} = \sum_{j \in \Phi_B \setminus 0} \hat{P} \beta^2 |h_j|^2 (\ell_j^2 + H_B^2)^{-\alpha/2}, \quad (5)$$

where h_j and d_j are the small scale fading channel and the distance between the typical user to the nearest BS, respectively. On the other hand, the aggregate interference from all IRSs can be modeled as follows:

$$\hat{I}_R = \sum_{j \in \Phi_B} \sum_{m=1}^M \hat{P} |\hat{\mathbf{g}}_{0,m}^H \Theta_m \hat{\mathbf{f}}_{m,j}|^2 = \sum_{j \in \Phi_B} \sum_{m=1}^M \hat{P} \left| \sum_{n=1}^N C_{m_n,j} f_{m_n,j} g_{0,m_n} e^{j\theta_{m_n}} \right|^2. \quad (6)$$

D. Power Consumption Model

We consider p_{BS} and p_U as the static power consumption of BS and user, respectively. The transmission power of BS in the direct mode is \hat{P} and indirect mode is P . The IRS is acting as a passive device and does not have any additional transmission power consumption. However, the IRS power consumption is associated with the number of IRS elements and the phase resolution [3] and can be written as $p_{IRS} = NP_r(b)$, where $P_r(b)$ denotes the phase resolution power consumption. The power consumption of the finite phase resolution, for instance, for 6 bits is $P_r(6) = 78$ mW which is much lower than the power consumption for infinite phase resolution $P_r(\infty) = 45$ dBm (Fig. 4 of [20]). Therefore, hardware power consumption increases with an increase in resolution and the number of IRS elements as provided in [3], [20]. The system power consumption per user in the IRS-assisted mode p_{ID} is given as $p_{ID} = p_{BS} + p_U + P + p_{IRS}$, whereas the power consumption of direct mode p_D is given as $p_D = p_{BS} + p_U + \hat{P}$.

E. Methodology of Analysis

To derive the coverage probability of different types of users in a large-scale IRS-assisted network, our methodology is as follows:

- **(IRS-assisted User)** Model the received signal power S_{R_0} as a sum of scaled generalized gamma random variables and then derive the LT of S_{R_0} (**Section III**).
- **(IRS-assisted User)** Derive the LT of the aggregate interference observed at a typical IRS-assisted user from all BSs, i.e., LT of I_B . Then, we model the aggregate interference observed at a typical IRS-assisted user from all IRSs as sum of normal random variables and derive its corresponding LT, i.e., LT of I_R (**Section IV**).
- Then, apply Gil-Pelaez inversion to obtain C_{ID} conditioned on the distance $r_{0,0}$ ¹.

¹We approximate $r_{0,0_n} \approx r_{0,0}$ since the distance between the typical user and different elements of the nearest IRS is almost the same, i.e., the distance between IRS elements is negligible compared to the distance between the nearest IRS and the typical user. Similarly $t_{0_n,j} \approx t_{0,j}$, $r_{0,m_n} \approx r_{0,m}$, and $t_{m_n,j} \approx t_{m,j}$.

- **(Direct User)** Derive the LT of \hat{I}_B and \hat{I}_R , i.e., $\mathcal{L}_{\hat{I}_B}(s)$ and $\mathcal{L}_{\hat{I}_R}(s)$, respectively, and obtain C_D conditioned on distance d_0 .
- Derive the ergodic capacity using Hamdi's lemma [21] and energy-efficiency of typical IRS-assisted user and direct user.

III. STATISTICS OF THE RECEIVED SIGNAL POWER (IRS-ASSISTED TRANSMISSION)

In what follows, we model the received power at a typical IRS-assisted user S_{R_0} as a sum of scaled generalized gamma random variables and derive the LT of S_{R_0} conditioned on $r_{0,0}$.

Lemma 1. *The desired signal power through nearest IRS $S_{R_0}(r_{0,0})$ in (1) can be modeled as a sum of scaled generalized gamma random variable as follows:*

$$S_{R_0} = Pr_{0,0}^{-\alpha} t_{0,j}^{-\alpha} \sum_{q=1}^{N^2} |a_q| X_{GG_q}(\zeta^2, 0.5\kappa, 0.5), \quad (7)$$

where $a_q = \cos(\beta_{0_n} - \beta_{0_k})$, $\forall q = 1, \dots, n+k, \dots, N^2$, $n = \{1, \dots, N\}$, $k = \{1, \dots, N\}$.

Proof. The desired signal power through nearest IRS $S_{R_0}(r_{0,0})$ in (1) is simplified using the following steps:

$$\begin{aligned} S_{R_0}(r_{0,0}) &= Pr_{0,0}^{-\alpha} t_{0,j}^{-\alpha} \left| \sum_{n=1}^N |f_{0_n,j}| |g_{0,0_n}| e^{-j\beta_{0_n}} \right|^2 \stackrel{(a)}{\approx} Pr_{0,0}^{-\alpha} t_{0,j}^{-\alpha} \left| \sum_{n=1}^N X_{G_n}(\kappa, \zeta) e^{-j\beta_{0_n}} \right|^2 \\ &\stackrel{(b)}{=} Pr_{0,0}^{-\alpha} t_{0,j}^{-\alpha} \sum_{n=1}^N \sum_{k=1}^N \cos(\beta_{0_n} - \beta_{0_k}) X_{G_n}(\kappa, \zeta) X_{G_k}(\kappa, \zeta) \\ &\stackrel{(c)}{=} Pr_{0,0}^{-\alpha} t_{0,j}^{-\alpha} \sum_{n=1}^N \sum_{k=1}^N \cos(\beta_{0_n} - \beta_{0_k}) X_{GG_{k,n}}(\zeta^2, 0.5\kappa, 0.5) \\ &\stackrel{(d)}{=} Pr_{0,0}^{-\alpha} t_{0,j}^{-\alpha} \sum_{q=1}^{N^2} |a_q| X_{GG_q}(\zeta^2, 0.5\kappa, 0.5), \end{aligned} \quad (8)$$

where $C_{0_n,j} \approx C_{0,j}$ (a) is followed by noting that $|g_{0,0_n}| |f_{0_n,j}|$ is the product of two independent Rayleigh distributed random variables with mean and variance $\mu_x = \sigma\pi/2$ and $\sigma_x^2 = 2^2\sigma^2(1 - \pi^2/16)$, respectively. However, the exact distribution of the product of two i.i.d Rayleigh random variables in [22] is complicated. Therefore, to maintain tractability, we approximate it as a gamma random variable $X_{G_n}(\kappa, \zeta)$ with the shape and scale parameter $\kappa = m = 1.6467$ and $\zeta = \frac{\Omega}{m} = 0.9539$, respectively [23]. Note that (b) follows from the simplification of (a) using $|x|^2 = \text{Re}(x)^2 + \text{Im}(x)^2$ and trigonometric identity $\cos(\alpha - \beta) = \cos(\alpha)\cos(\beta) - \sin(\alpha)\sin(\beta)$. Next,

(c) follows from the fact that the product of two i.i.d gamma random variables is equivalent to generalized gamma random variable $X_{GG_q}(a, d, p)$, where $a = \zeta^2$, $d = \frac{\kappa}{2}$, and $p = \frac{1}{2}$ represent the scale, shape, and power, respectively [24]. Finally, in (d), the double summation $n = 1, \dots, N$, $k = 1, \dots, N$ and $a_q = \cos(\beta_{0_n} - \beta_{0_k})$ is transformed to single summation $q = 1, \dots, n + k, \dots, N^2$, where $-\pi/2 \leq \beta_{0_n} - \beta_{0_k} \leq \pi/2$. \square

In what follows, we derive the conditional LT of the received signal power in the IRS-assisted communication mode.

Lemma 2. *Conditioned on $r_{0,0}$, the LT of the S_{R_0} experienced by the typical user through nearest IRS $\mathcal{L}_{S_{R_0}}$ in the IRS-assisted indirect communication mode is given as follows:*

$$\mathcal{L}_{S_{R_0}|r_{0,0}}(s) = \mathbb{E} \left[\prod_{q=1}^{N^2} \frac{1}{(2\zeta^2 s \hat{a}_q)^d} \exp \left(\frac{1}{8 \zeta^2 s \hat{a}_q} \right) D_{-2d} \left(\frac{1}{2\zeta^2 s \hat{a}_q} \right) \right], \quad (9)$$

where $\hat{a}_q = Pr_{0,0}^{-\alpha} t_{0,j}^{-\alpha} a_q$, a_q is defined in Lemma 1 and $D_{-v}(\cdot)$ is the parabolic cylinder function.

Proof. The LT of S_{R_0} is given by using step (d) of (8) as follows:

$$\begin{aligned} \mathcal{L}_{S_{R_0}|r_{0,0}}(s) &= \mathbb{E}[e^{-sS_{R_0}}] \\ &= \mathbb{E}[e^{-sPr_{0,0}^{-\alpha} t_{0,j}^{-\alpha} \sum_{q=1}^{N^2} a_q X_{GG_q}(\zeta^2, 0.5\kappa, 0.5)}] \\ &= \prod_{q=1}^{N^2} \mathbb{E}[e^{-sPr_{0,0}^{-\alpha} t_{0,j}^{-\alpha} a_q X_{GG_q}(\zeta^2, 0.5\kappa, 0.5)}], \end{aligned} \quad (10)$$

where (10) follows from the fact that MGF of the linear combination of independent variables can be rewritten as the product of MGFs of each of the independent variables, and

$$\begin{aligned} \mathbb{E}[e^{-sPr_{0,0}^{-\alpha} t_{0,j}^{-\alpha} a_q X_{GG_q}(\zeta^2, 0.5\kappa, 0.5)}] &= \int_0^\infty e^{-s\hat{a}_q X_{GG_q}} f_{X_{GG}}(x) dx \\ &\stackrel{(a)}{=} \int_0^\infty \frac{0.5}{\zeta^\kappa \Gamma(\kappa)} x^{0.5\kappa-1} e^{-s\hat{a}_q x - \sqrt{\frac{x}{\zeta^2}}} dx \\ &\stackrel{(b)}{=} \frac{2}{\zeta^\kappa \Gamma(\kappa)} \int_0^\infty g^{\kappa-1} e^{-s\hat{a}_q g^2 - \frac{g}{\zeta}} dg \\ &\stackrel{(c)}{=} \frac{1}{(2\zeta^2 s \hat{a}_q)^{0.5\kappa}} \exp \left(\frac{1}{8 \zeta^2 s \hat{a}_q} \right) D_{-\kappa} \left(\frac{1}{2\zeta^2 s \hat{a}_q} \right), \end{aligned} \quad (11)$$

where (a) is obtained by substituting the probability density function of GG random variable $f_{X_{GG}}(x) = \frac{0.5}{\zeta^\kappa \Gamma(\kappa)} x^{0.5\kappa-1} e^{-\sqrt{\frac{x}{\zeta^2}}}$ [23], (b) is obtained by changing variable $g = \sqrt{x}$, (c) is derived by using the identity $\int_0^\infty g^{\nu-1} e^{-\beta g^2 - \gamma g} dg = (2\beta)^{-\frac{\nu}{2}} \Gamma[\nu] \exp(\frac{\gamma^2}{8\beta}) D_{-\nu} \left(\frac{\gamma}{\sqrt{2\beta}} \right)$ from Eq. 3.462 of

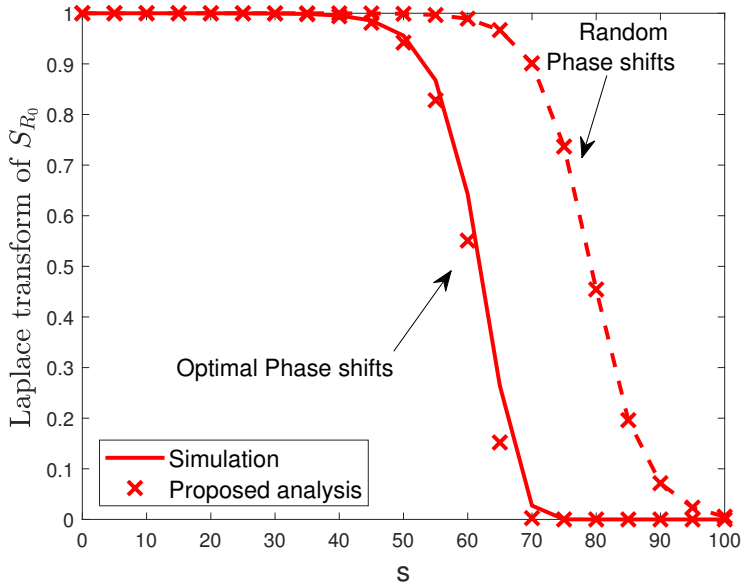


Fig. 2. Validation of conditional LT in (7) of the desired received signal power $S_{R_0}(r_0)$ considering (i) random IRS phase shifts and (ii) optimal IRS phase shifts obtained from CVX, using Monte-Carlo simulations.

[25], where $D_{-\nu}(\cdot)$ represents the parabolic cylinder function. Finally, by using $\hat{a}_q = Pr_{0,0}^{-\alpha} t_{0,j}^{-\alpha} a_q$ in step (c) of (11) and (10) results in **Lemma 2**. \square

Fig. 2 validates the accuracy of the LT of the received signal power (derived in **Lemma 2**) of the typical IRS-assisted user with the Monte-Carlo simulations. Our derived expressions match well with the simulations confirming the accuracy of our S_{R_0} model and its corresponding LT. In both Lemma 2 and simulations, the phase-shifts are obtained optimally from CVX. Specifically, we solve the following problem (**P1**) to maximize the received signal power (given in (1)) and obtain the optimal phase-shifts:

$$\begin{aligned} \mathbf{P1} : \max_{\theta_{0n}, \forall n} S_{R_0} &= P \left| \sum_{n=1}^N C_{0n,j} f_{0n,j} g_{0,0n} e^{j\theta_{0n}} \right|^2 \\ \text{s.t. } 0 &\leq \theta_{0n} \leq \pi, \forall n = 1, \dots, N., \end{aligned} \quad (12)$$

Substituting $f_{0n,j} = |f_{0n,j}| e^{-j\psi_{0n,j}}$, $g_{0,0n} = |g_{0,0n}| e^{-j\phi_{0,0n}}$, $\Theta_0 = \text{diag}\{e^{j\theta_{01}}, e^{j\theta_{02}}, \dots, e^{j\theta_{0N}}\}$ and $C_{0n,j} \approx C_{0,j} = r_{0,0}^{-\alpha} t_{0,j}^{-\alpha}$ defined in Sec. IIB, the objective function can be rewritten as $Pr_{0,0}^{-\alpha} t_{0,j}^{-\alpha} \left| \sum_{n=1}^N |f_{0n,j}| |g_{0,0n}| e^{-j\beta_{0n}} \right|^2$. Since $Pr_{0,0}^{-\alpha} t_{0,j}^{-\alpha}$ is independent of the optimization variable, we can discard this term. Now, we transform the objective to equivalent matrix form

as $|\tilde{\mathbf{g}}_{0,0}^H \mathbf{B}_0 \tilde{\mathbf{f}}_{0,j}|^2$, where $\tilde{\mathbf{g}}_{0,0} \in \mathbb{R}^{1 \times N}$, $\tilde{\mathbf{f}}_{0,j} \in \mathbb{R}^{N \times 1}$, and $\mathbf{B}_0 = \text{diag}\{e^{j\beta_{01}}, e^{j\beta_{02}}, \dots, e^{j\beta_{0N}}\}$. Since the objective function is a scalar, we can convert absolute square to norm square as $\|\tilde{\mathbf{g}}_{0,0}^H \mathbf{B}_0 \tilde{\mathbf{f}}_{0,j}\|^2$. Finally, defining $\mathbf{v} = [v_1, \dots, v_N]^H$, where $v_n = e^{j\beta_{0n}}, \forall n$, and $\Phi = \text{diag}(\tilde{\mathbf{g}}_{0,0}^H) \tilde{\mathbf{f}}_{0,j}$, we reformulate $\|\tilde{\mathbf{g}}_{0,0}^H \mathbf{B}_0 \tilde{\mathbf{f}}_{0,j}\|^2 = \|\mathbf{v}^H \Phi\|^2$. The problem **P1** can thus be reformulated as follows:

$$\begin{aligned} \mathbf{P2} : \max_{\mathbf{v}} \quad & \mathbf{v}^H \Phi \Phi^H \mathbf{v} \\ \text{s.t.} \quad & |v_n|^2 = 1, \forall n = 1, \dots, N. \end{aligned} \quad (13)$$

P2 is non-convex quadratically constrained quadratic program (QCQP) in the homogeneous form and the constraint is rank one [26]. Now, defining $\mathbf{V} = \mathbf{v}\mathbf{v}^H$, we apply semi-definite relaxation (SDR) to relax the constraint as follows:

$$\begin{aligned} \mathbf{P3} : \max_{\mathbf{V}} \quad & \text{Tr}(\Phi \Phi^H \mathbf{V}) \\ \text{s.t.} \quad & \mathbf{V}_{n,n} = 1, \forall n = 1, \dots, N, \quad \mathbf{V} \geq 0. \end{aligned} \quad (14)$$

Since the problem is now transformed in to a convex semidefinite program (SDP), similar to [27], we solve it for the optimal value using CVX.

Furthermore, Fig. 2 also compares the LT of S_{R_0} with optimal IRS phase-shifts to LT of S_{R_0} with random IRS phase shifts. For a given value of s , the LT of S_{R_0} with optimal IRS phase-shifts is lower than the LT of S_{R_0} with random IRS phase-shifts. Thus, it is evident that the received signal power S_{R_0} with optimal phase-shifts significantly outperforms the received signal power S_{R_0} with random phase shifts.

As a special case of **Lemma 2** for optimal phase-shifts, the statistics of the received signal power can be modeled as follows.

Corollary 1. *The optimal received signal power can be obtained if we substitute $\beta_{0n,j} = \theta_{0n} - \psi_{0n,j} - \phi_{0,0n} = 0$ in (7), which maximizes a_q to unity $\forall n \in \{1, \dots, N\}$ [5] and results in maximum S_{R_0} as $S_{R_0} = Pr_{0,0}^{-\alpha} t_{0,j}^{-\alpha} W$. In this case, $W = \sum_{q=1}^{N^2} X_{GG_q}(\zeta^2, 0.5\kappa, 0.5)$ can be modeled as a normal random variable Since the square of the number of IRS elements can be a large number, using CLT with mean $\mu_w = N^2 \mu_{GG}$ and variance $\sigma_w^2 = N^2 \sigma_{GG}^2$. where $\mu_{GG} = \zeta^2 \frac{\Gamma(\kappa+2)}{\Gamma(\kappa)}$ and $\sigma_{GG} = \zeta^4 \left(\frac{\Gamma(\kappa+4)}{\Gamma(\kappa)} - \mu_{GG}^2 \right)$ [24], we have the mean and the variance of S_{R_0} as $\mathbb{E}[S_{R_0}] = Pr_{0,0}^{-\alpha} t_{0,j}^{-\alpha} \mu_{GG}$ and $\mathbb{V}[S_{R_0}] = P^2 r_{0,0}^{-2\alpha} t_{0,j}^{-2\alpha} \sigma_{GG}$, respectively.*

IV. STATISTICS OF THE AGGREGATE INTERFERENCE (IRS-ASSISTED TRANSMISSION)

In this section, we first derive the LT of the aggregate interference observed at a typical IRS-assisted user from all BSs. Then, we model the worst-case aggregate interference observed at a

typical IRS-assisted user from all IRSs and derive its corresponding LT.

The LT of the aggregate interference observed at a typical IRS-assisted user from all BSs (excluding the blocked nearest direct BS) $\mathcal{L}_{I_B}(s)$ is derived as follows:

$$\begin{aligned}
\mathcal{L}_{I_B|d_0}(s) &= \mathbb{E}[e^{-s \sum_{j \in \Phi_B \setminus 0} P \beta^2 |h_j|^2 (\ell_j^2 + H_B^2)^{-\alpha/2}}] \\
&\stackrel{(a)}{=} \mathbb{E}_{\Phi_B} \left[\prod_{j \in \Phi_B \setminus 0} \frac{1}{1 + s P \beta^2 (\ell_j^2 + H_B^2)^{-\alpha/2}} \right] \\
&\stackrel{(b)}{=} \exp \left(-2\pi \lambda_B \int_{\ell_0}^{\infty} \left(1 - \frac{1}{1 + P \beta^2 (\ell_j^2 + H_B^2)^{-\alpha/2}} \right) \ell_j d\ell_j \right) \\
&\stackrel{(c)}{=} \exp \left(-2\pi \lambda_B \int_{d_0}^{\infty} \left(1 - \frac{1}{1 + P \beta^2 d_j^{-\alpha}} \right) d_j dd_j \right),
\end{aligned} \tag{15}$$

where (a) is obtained by applying the LT of $|h_j|^2$ and $|h_j|^2 \sim \exp(1)$, and (b) is derived using PGFL w.r.t the two-dimensional distance ℓ_j of the interfering BSs [18], and (c) is obtained by substituting $d_j = \sqrt{\ell_j^2 + H_B^2}$. The closed-form expression can then be obtained as follows:

$$\mathcal{L}_{I_B|d_0}(s) = \exp \left(-2\pi \lambda_B \frac{d_0^{2-\alpha} s P \beta^2}{\alpha - 2} {}_2F_1 \left(1, \frac{-2 + \alpha}{\alpha}; 2 - \frac{2}{\alpha}; -s P \beta^2 d_0^{-\alpha} \right) \right). \tag{16}$$

Corollary 2. For $\alpha = 4$, the LT of the aggregate interference to the typical user through all the BSs (except the associated BS₀) $\mathcal{L}_{\hat{I}_B}$ in the direct mode can be simplified as:

$$\mathcal{L}_{\hat{I}_B|d_0}(s) = \exp \left(-\pi \lambda_B \sqrt{s P \beta^2} \arctan \left(\sqrt{s \hat{P} \beta^2 d_0^{-4}} \right) \right),$$

using ${}_2F_1(1, 0.5; 1.5; -X^2) = \frac{\arctan X}{X}$, for $|X| < 1$ [28][Eq. 15.4.3].

Lemma 3 (Lower Bound on the Aggregate Interference from Multiple IRSs). *We reformulate the aggregate interference observed at a typical user from all IRSs (excluding nearest IRS) in a multi-IRS, multi-BS scenario as $I_R \leq \sum_{j \in \Phi_B} P Z_j$, where $Z_j = \sum_{m=1}^{M-1} r_{0,m}^{-\alpha} t_{m,j}^{-\alpha} Y_m$.*

Proof. Taking $\beta_{m_n,j} = \theta_{m_n} - \psi_{m_n,j} - \phi_{0,m_n}$, the I_R expression in (3) can be rewritten as follows:

$$\begin{aligned}
I_R &\stackrel{(a)}{=} \sum_{j \in \Phi_B} P \sum_{m=1}^{M-1} r_{0,m}^{-\alpha} t_{m,j}^{-\alpha} \left| \sum_{n=1}^N |f_{m_n,j}| |g_{0,m_n}| e^{j \beta_{m_n,j}} \right|^2 \\
&\stackrel{(b)}{\leq} \sum_{j \in \Phi_B} P \sum_{m=1}^{M-1} r_{0,m}^{-\alpha} t_{m,j}^{-\alpha} \left| \sum_{n=1}^N |f_{m_n,j}| |g_{0,m_n}| \right|^2 \\
&\stackrel{(c)}{=} \sum_{j \in \Phi_B} P \sum_{m=1}^{M-1} r_{0,m}^{-\alpha} t_{m,j}^{-\alpha} Y_m \stackrel{(d)}{=} \sum_{j \in \Phi_B} P Z_j,
\end{aligned} \tag{17}$$

where (a) is obtained by substituting $C_{m_n,j} = (r_{0,m_n} t_{m_n,j})^{-\alpha/2}$ and considering the approximation $r_{0,m} \approx r_{0,m_n}$, $t_{m,j} \approx t_{m_n,j}$ as discussed in footnote-1, (b) follows from $\beta_{m_n,j} = \theta_{m_n} - \psi_{m_n,j} - \phi_{0,m_n} = 0$ which results in the maximum interference (excluding nearest IRS) and hence referred to as *worst case interference*. Finally, step (c) and step (d) follow by defining $Y_m = |\sum_{n=1}^N |f_{m_n,j}| |g_{0,m_n}||^2$ and $Z_j = \sum_{m=1}^{M-1} r_{0,m}^{-\alpha} t_{m,j}^{-\alpha} Y_m$, respectively. \square

In what follows, we derive the statistics of the aggregate interference observed at a typical user from multiple IRSs in a multi-BS scenario.

Lemma 4 (Distribution of the Aggregate Interference from Multiple IRSs (Excluding the Nearest IRS) in a Multi-BS Scenario). *Leveraging the results in Lemma 3, given $I_R \leq \sum_{j \in \Phi_B} P Z_j$, where $Z_j = \sum_{m=1}^{M-1} r_{0,m}^{-\alpha} t_{m,j}^{-\alpha} Y_m$ follows a Normal distribution with mean and variance given by*

$$\mu_{Z_j} = \mathbb{E}[r_{0,m}^{-\alpha}] ((M-1)t_j^2)^{-\alpha/2} (1+\lambda) \quad \text{and} \quad \sigma_{Z_j}^2 = 2\mathbb{V}[r_{0,m}^{-\alpha}] ((M-1)t_j^2)^{-\alpha} (1+2\lambda),$$

and Y_m represents the non-central Chi-square random variable with mean and variance $\mu_Y = (1+\lambda)$ and $\sigma_Y^2 = 2(1+2\lambda)$, respectively.

Proof. Let $X_n = |g_{0,m_n}| |f_{m_n,j}|$ denote the product of two independent Rayleigh distributed random variables with mean and variance $\mu_x = \sigma\pi/2$ and $\sigma_x^2 = 2^2\sigma^2(1-\pi^2/16)$, respectively [29]. Since the IRS elements are typically large, we leverage on central limit theorem (CLT) to depict $X' = \sum_{n=1}^N X_n$ follows a normal distribution with the mean and variance given by $\mu_{X'} = N\mu_x$ and $\sigma_{X'}^2 = N\sigma_x^2$, respectively. We refer to this approximation as *Level-1 Gaussian approximation*. Consequently, $Y_m = |\sum_{n=1}^N X_n|^2$ will follow a non-central chi-square distribution with unity degree of freedom $\nu = 1$ and non-centrality parameter $\lambda = \frac{1}{2} \frac{\mu_{X'}^2}{\sigma_{X'}^2}$ [29]. Therefore, the mean and variance of Y_m can be obtained as in **Lemma 4**.

Let $Y'_m = r_{0,m}^{-\alpha} t_{m,j}^{-\alpha} Y_m$ denote the product of three random variables $t_{m,j}^{-\alpha}$, $r_{0,m}^{-\alpha}$, and Y_m , where $t_{m,j}^{-\alpha}$, and $r_{0,m}^{-\alpha}$ are correlated by cosine law as $t_{m,j}^{-\alpha} = (r_{0,m}^2 + d_j^2 - 2r_{0,m}d_j \cos \psi_m)^{-\alpha/2}$ [17], [30]. To simplify the analysis, we propose an alternate formulation of $t_{m,j}$, i.e., instead of using cosine law we alternatively define $t_{m,j} = \sqrt{\ell_{m,j}^2 + (H_B - H_R)^2}$ (refer to the triangle in Fig. 3(b)). Next, to enhance tractability, we consider that the typical IRS is located in the middle of the BS_j and typical user (i.e., $\ell_{m,j} \approx \frac{\ell_j}{2}$) which upon substitution gives

$$t_{m,j} \approx t_j = \sqrt{\left(\frac{\ell_j}{2}\right)^2 + (H_B - H_R)^2}. \quad (18)$$

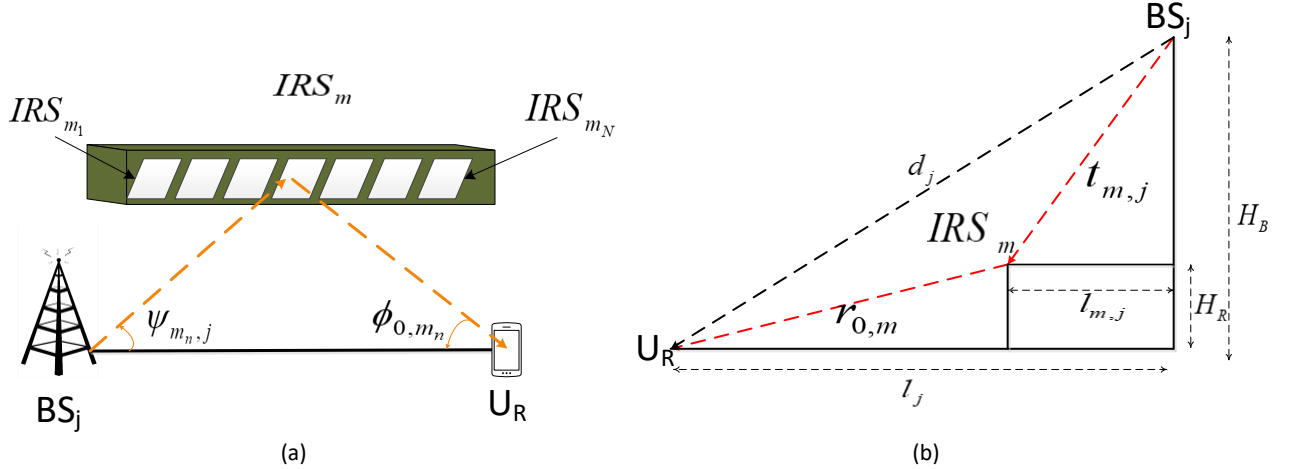


Fig. 3. (a): Zoomed view of IRS functionality as a reflector, and (b) triangle explaining the IRS distance approximation.

Subsequently, we have $Y'_m \approx r_{0,m}^{-\alpha} t_j^{-\alpha} Y_m$, and $Z = \sum_{m=1}^{M-1} Y'_m$ will follow a normal distribution using CLT as shown in **Lemma 4**. We refer to this as *Level-2 Gaussian approximation*. \square

The factor $r_{0,m}^{-\alpha} t_{m,j}^{-\alpha}$ is important in modeling Y'_m as is evident in **Lemma 4**. Note that $r_{0,m}^{-\alpha}$ and $t_{m,j}^{-\alpha}$ are correlated using cosine law. However, Fig. 4 shows that the correlation is weak and thus the approximation in (18) is accurate. In the sequel, we first compare $\mathbb{E}[r_{0,m}^{-\alpha}] \mathbb{E}[t_{m,j}^{-\alpha}]$, and $\mathbb{E}[r_{0,m}^{-\alpha} t_j^{-\alpha}]$ to show the weak correlation. Then, we demonstrate the validity of the proposed approximation $\mathbb{E}[r_{0,m}^{-\alpha}] \mathbb{E}[t_j^{-\alpha}]$ to validate its accuracy in Fig. 4. It is also clear from the figure that λ_R does not have any impact on the distances $t_{m,j}$ and $r_{0,m}$ on average. It is clear from the right figure that increase in path-loss exponent α causes an increase in the path-loss distance term and hence decreases in $\mathbb{E}[r_{0,m}^{-\alpha}] \mathbb{E}[t_{m,j}^{-\alpha}]$, $\mathbb{E}[r_{0,m}^{-\alpha} t_j^{-\alpha}]$ and $\mathbb{E}[r_{0,m}^{-\alpha}] \mathbb{E}[t_j^{-\alpha}]$ are evident. In what follows, we derive the first and second moment of $r_{0,m}^{-\alpha}$ as is required in **Lemma 4**.

Lemma 5. *The i -th moment of the random variable $r_{0,m}^{-\alpha}$ can be derived for finite values of R and when $R \rightarrow \infty$, respectively, as follows:*

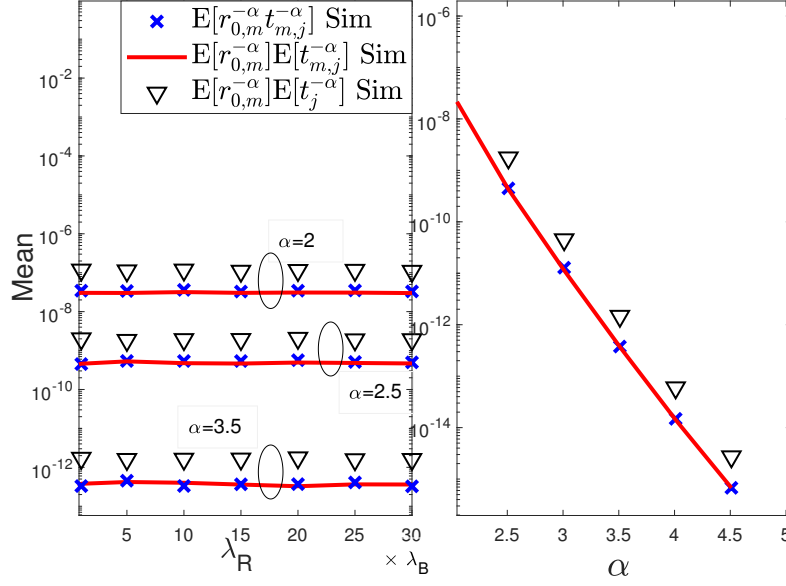


Fig. 4. Comparison of $\mathbb{E}[r_{0,m}^{-\alpha} t_{m,j}^{-\alpha}]$, $\mathbb{E}[r_{0,m}^{-\alpha}] \mathbb{E}[t_{m,j}^{-\alpha}]$ and the proposed approximation of $\mathbb{E}[r_{0,m}^{-\alpha}] \mathbb{E}[t_j^{-\alpha}]$ in (18).

$$\begin{aligned}
 \mathbb{E}[(r_{0,m}^{-\alpha})^i] &= \int_0^R r_{0,m}^{-i\alpha} \frac{\ell_m^2}{\pi R^2} d\ell_m = \int_{\ell_m=0}^R (\ell_m^2 + H_R^2)^{-\frac{i\alpha}{2}} \frac{\ell_m^2}{\pi R^2} d\ell_m \\
 &= \frac{-2(H_R^2 + R^2)^{-1-\frac{i\alpha}{2}}}{(-2+i\alpha)R^2} + \frac{2H_R^{2-i\alpha}}{(-2+i\alpha)R^2} \\
 \lim_{R \rightarrow \infty} \mathbb{E}[(r_{0,m}^{-\alpha})^i] &= \frac{2(H_R)^{2-i\alpha}}{(-2+i\alpha)R^2}.
 \end{aligned} \tag{19}$$

Finally, we derive the LT of the interference experienced by the typical user from all IRSs to compute the coverage probability.

Lemma 6. *The LT of interference experienced by the typical user through the all IRSs (except nearest IRS to the typical user) \mathcal{L}_{I_R} in the IRS- assisted communication mode is given as follows:*

$$\mathcal{L}_{I_R|r_{0,0}}(s) \approx \exp \left(2\pi\lambda_B \frac{4}{\alpha} \sum_{i=1}^{\infty} \frac{b_i(s)}{i - \frac{2}{\alpha}} \left(X_R^{i-\frac{2}{\alpha}} - X_0^{i-\frac{2}{\alpha}} \right) \right), \tag{20}$$

where $b_i(s)$ denotes the Taylor's series expansion coefficients of $\exp(-k_1(s)x - k_2(s)x^2)$ and $k_1(s) = \mu_{Z_j} s P / t_j^{-\alpha}$, and $k_2(s) = \frac{1}{2t_j^{-2\alpha}} \sigma_{Z_j}^2 s^2 P^2$.

Proof. Using (17) in (3), we derive LT $\mathcal{L}_{I_R}(s)$ as:

$$\begin{aligned}
\mathcal{L}_{I_R|r_{0,0}}(s) &= \mathbb{E}[e^{-sI_R}] = \mathbb{E}[e^{-s\sum_{j\in\Phi_B} PZ_j}] = \mathbb{E}\left[\prod_{j\in\Phi_B} e^{-sPZ_j}\right] \\
&\stackrel{(a)}{=} \mathbb{E}\left[\prod_{j\in\Phi_B} \mathbb{E}_Z[e^{-sPZ_j}]\right] = \mathbb{E}\left[\prod_{j\in\Phi_B} e^{-(\mu_{Z_j}sP + \frac{1}{2}\sigma_{Z_j}^2s^2P^2)}\right] \\
&\stackrel{(b)}{=} \exp\left(-2\pi\lambda_B \int_0^R \left(1 - e^{-(k_1(s)t^{-\alpha} + k_2(s)t^{-2\alpha})}\right) \ell d\ell\right) \\
&\stackrel{(c)}{=} \exp\left(-2\pi\lambda_B \frac{-4}{\alpha} \int_{X_0}^{X_R} \left(1 - e^{-(k_1(s)X + k_2(s)X^2)}\right) X^{-\frac{2}{\alpha}-1} dX\right) \\
&\stackrel{(d)}{=} \exp\left(2\pi\lambda_B \frac{4}{\alpha} \int_{X_0}^{X_R} \sum_{i=1}^{\infty} b_i(s) X^{i-\frac{2}{\alpha}-1} dX\right) \\
&\stackrel{(e)}{=} \exp\left(2\pi\lambda_B \frac{4}{\alpha} \sum_{i=1}^{\infty} \frac{b_i(s)}{i - \frac{2}{\alpha}} \left(X_R^{i-\frac{2}{\alpha}} - X_0^{i-\frac{2}{\alpha}}\right)\right),
\end{aligned} \tag{21}$$

where (a) follows from the LT of Z_j where Z_j is a Gaussian random variable with μ_{Z_j} , and $\sigma_{Z_j}^2$ is given by **Lemma 4**, (b) follows by substituting $k_1(s) = \mu_{Z_j}sP/t_j^{-\alpha}$ and $k_2(s) = \frac{1}{2t_j^{2\alpha}}\sigma_{Z_j}^2s^2P^2$ and then we apply PGFL w.r.t ℓ_j where $t = \sqrt{\left(\frac{\ell}{2}\right)^2 + (H_B - H_R)^2}$ and t_j is given in (18). For simplicity, (c) is obtained by changing of variable ℓ to X , i.e., $X = \left(\frac{\ell^2}{4} + (H_B - H_R)^2\right)^{-\alpha/2}$, where $X_0 = (H_B - H_R)^{-\alpha}$ and $X_R = \left(\frac{R^2}{4} + (H_B - H_R)^2\right)^{-\alpha/2}$. Note that (d) is obtained by using Taylor's series expansion of $\exp(-k_1x - k_2x^2)$ and $b_i(s)$ denotes the coefficients of the expanded Taylor series. Finally, (e) is obtained by solving the integral. \square

Fig. 5 validates the accuracy of LT of aggregate interference from IRSs for different number of IRSs, i.e., $M = 300$ and $M = 1500$ and transmission power $P = 1$ W and $P = 20$ W. This figure shows that, for a given value of s , increasing transmission power and IRS intensity decreases IRS interference. Clearly, the interference in higher power and higher intensity trend dominates compared to all other combinations of power and IRS intensity. Similarly, Fig. 6 validates the accuracy of the LT of the aggregate interference from BSs (excluding the nearest BS) given in (16) as a function of s . Again, the LT of aggregate interference decreases with increasing transmission power of BSs (i.e., the interference increases). Unlike Fig. 5, neither the IRS intensity nor the total number of IRSs M have any effect on \mathcal{L}_{I_B} as the direct transmissions are independent of λ_R or M .

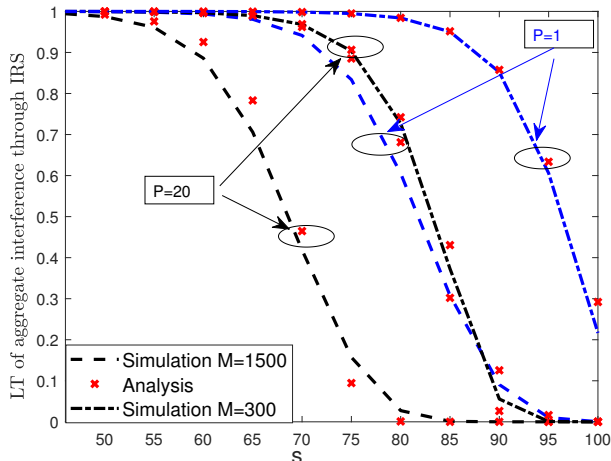


Fig. 5. Conditional LT of aggregate interference from IRSs (excluding the nearest IRS), $\mathcal{L}_{I_R}(s)$ in (20), for $\lambda_R = 2\lambda_0$, $M = 300$ and $\lambda_R = 10\lambda_0$, $M = 1500$ with $P = 1$ and $P = 20$, using Monte-Carlo simulations.

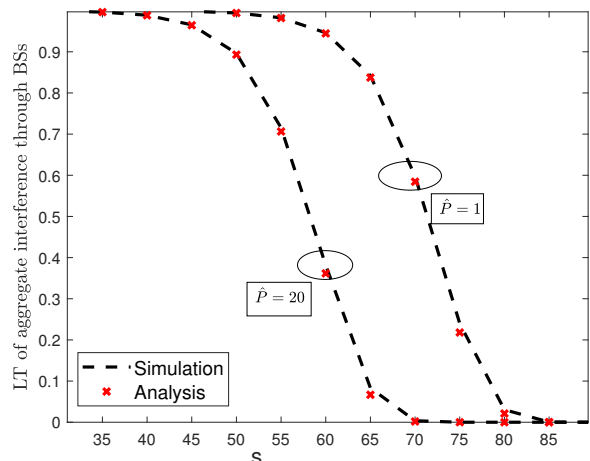


Fig. 6. Conditional LT of aggregate interference from BSs (excluding the nearest BS in direct mode), $\mathcal{L}_{I_B}(s)$ (16), for $\hat{P} = P = 1$, $\hat{P} = P = 20$, and $\lambda_R = 2\lambda_0$, $M = 300$, using Monte-Carlo simulations.

V. COVERAGE PROBABILITY AND ERGODIC CAPACITY CHARACTERIZATION

In this section, we first derive the coverage probability of an IRS-assisted user and then the coverage probability of users who are supported by direct transmissions. Then, we derive the ergodic capacity and energy efficiency of an IRS-assisted user and the user supported by direct transmission from BS. Finally, we derive the overall network coverage, ergodic rate, and energy-efficiency considering the fraction of IRS-assisted and direct users in the network.

A. Coverage Probability (IRS-assisted Transmission)

The coverage probability of the typical user associated to nearest IRS in the IRS-assisted indirect mode of communication is defined as $C_{ID} = \Pr(\gamma_{ID} \geq \tau)$, where the SINR for IRS-assisted indirect transmission is given as follows:

$$\gamma_{ID} = \frac{S_{R_0}}{I_B + I_R + N_0}. \quad (22)$$

The coverage probability can be calculated numerically by using Gil-Paleaz inversion theorem [31] as shown in the following:

$$\begin{aligned}
C_{\text{ID}} &= \Pr(\gamma_{\text{ID}} \geq \tau) \\
&= \Pr(S_{R_0}(r_{0,0}) - \tau I_R \geq \tau I_B + \tau N_0) = \Pr(\Omega \geq \tau I_B + \tau N_0) \\
&= \mathbb{E}_{r_{0,0}} \left[\frac{1}{2} - \frac{1}{\pi} \int_0^\infty \frac{\text{Im}[\phi_{\Omega|r_{0,0}}(\omega) \mathcal{L}_{I_B}(-j\omega\tau) e^{j\omega\tau N_0}]}{\omega} d\omega \right] \\
&= \frac{1}{2} - \frac{1}{\pi} \int_0^\infty \frac{\text{Im}[\phi_{\Omega}(\omega) \mathcal{L}_{I_B}(-j\omega\tau) e^{j\omega\tau N_0}]}{\omega} d\omega,
\end{aligned} \tag{23}$$

where

$$\phi_{\Omega}(\omega) = \mathbb{E}_{r_{0,0}}[\phi_{\Omega|r_{0,0}}(\omega)] = \mathbb{E}_{r_{0,0}}[e^{-j\omega\Omega}] = \mathbb{E}_{r_{0,0}}[\mathcal{L}_{S_{R_0}|r_{0,0}} \mathcal{L}_{I_R|r_{0,0}}(-j\omega\tau)]. \tag{24}$$

Note that $\mathcal{L}_{I_B}(-j\omega\tau) = \mathbb{E}_{d_0}[\mathcal{L}_{I_B|d_0}(-j\omega\tau)]$ is independent of $r_{0,0}$. Substituting (20) and (9) in (24) and then substituting (24) and (16) in (23), we obtain C_{ID} . The distribution of the distance of the nearest IRS at height H_R to the typical user is given as follows [32]:

$$f_{r_0}(r_{0,0}) = \frac{2Mr_{0,0}}{R^2} \left(1 - \frac{r_{0,0}^2 - H_R^2}{R^2} \right)^{M-1}. \tag{25}$$

Also, the distance of the nearest BS at height H_B to the typical user is given as:

$$f_{d_0}(d_0) = 2\pi\lambda_B d_0 e^{-\pi\lambda_B(d_0^2 - H_B^2)}. \tag{26}$$

B. Coverage Probability (Direct Transmission)

The coverage probability of the typical user with the direct mode of communication is defined as $C_D = \Pr(\gamma_D \geq \tau)$, where the SINR of the direct communication mode is given as

$$\gamma_D = \frac{S_{D_0}}{\hat{I}_B + \hat{I}_R + N_0}. \tag{27}$$

Now by substituting (4), the coverage probability C_D can be written as follows:

$$\begin{aligned}
C_D &= \Pr\left(|h_0|^2 \geq d_0^\alpha \frac{\tau\beta^{-2}}{\hat{P}} \left(\hat{I}_B + \hat{I}_R + N_0\right)\right) \\
&= \mathbb{E}_{d_0} \left[e^{-\frac{\tau d_0^\alpha N_0}{\beta^2 \hat{P}}} \mathcal{L}_{\hat{I}_B} \left(\frac{\tau d_0^\alpha}{\beta^2 \hat{P}} \right) \mathcal{L}_{\hat{I}_R} \left(\frac{\tau d_0^\alpha}{\beta^2 \hat{P}} \right) \right],
\end{aligned} \tag{28}$$

where $\mathcal{L}(\cdot)$ is the LT and d_0 is the distance between the typical user and the nearest BS, i.e., $d_0 = \sqrt{\ell_0^2 + H_B^2}$. The distribution of the distance of the nearest BS is provided in (26).

Corollary 3. *The LT of the aggregate interference to the typical user through all the BSs (except the associated BS₀) $\mathcal{L}_{\hat{I}_B}$ in the direct mode can then be obtained as follows:*

$$\mathcal{L}_{\hat{I}_B|d_0}(s) = \exp\left(-2\pi\lambda_B \frac{d_0^{2-\alpha} s \hat{P} \beta^2}{\alpha - 2} {}_2F_1\left(1, \frac{-2 + \alpha}{\alpha}; 2 - \frac{2}{\alpha}; -s \hat{P} \beta^2 d_0^{-\alpha}\right)\right), \quad (29)$$

which is similar to (16) with P replaced with \hat{P} for the direct mode.

Corollary 4. *Similar to Lemma 6, the LT of interference experienced by the typical user through the all the IRSs and all the BSs $\mathcal{L}_{\hat{I}_R}$ in direct communication mode is given as follows:*

$$\mathcal{L}_{\hat{I}_R}(s) \approx \exp\left(2\pi\lambda_B \frac{4}{\alpha} \sum_{i=1}^{\infty} \frac{\hat{b}_i(s)}{i - \frac{2}{\alpha}} \left(X_R^{i - \frac{2}{\alpha}} - X_0^{i - \frac{2}{\alpha}}\right)\right), \quad (30)$$

where $\hat{b}_i(s)$ denotes the Taylor's series expansion coefficients of $\exp(-\hat{k}_1(s)x - \hat{k}_2(s)x^2)$ and $\hat{k}_1(s) = \hat{\mu}_{Z_j} s \hat{P} / t_j^{-\alpha}$, and $\hat{k}_2(s) = \frac{1}{2t_j^{2\alpha}} \hat{\sigma}_{Z_j}^2 s^2 \hat{P}^2$, $\hat{\mu}_{Z_j} = \mathbb{E}[r_{0,m}^{-\alpha}] (Mt_j^2)^{-\alpha/2} (1 + \lambda)$ and $\hat{\sigma}_{Z_j}^2 = 2\mathbb{V}[r_{0,m}^{-\alpha}] (Mt_j^2)^{-\alpha} (1 + 2\lambda)$.

Note that the difference arises from the fact that \hat{I}_R has M interfering IRSs in **Corollary 4**, whereas in **Lemma 4**, we have $M - 1$ IRSs contributing to the aggregate interference I_R . Finally, substituting (29) and (30) in (28), we obtain the coverage probability of direct link C_D conditioned on the distance d_0 .

C. Ergodic Capacity

The achievable ergodic capacity of a typical user can be given by using the coverage probability expressions as shown below [33]:

$$\mathbb{E}[\log_2(1 + \text{SINR})] = \frac{1}{\ln(2)} \int_0^{\infty} \frac{P(\text{SINR} > t)}{t} dt.$$

However, the aforementioned evaluation adds one more layer of integration on top of the coverage probability. Therefore, we use an alternative LT-based approach to evaluate ergodic capacity by leveraging on Hamdi's lemma [21] given as follows:

$$\mathbb{E}\left[\ln\left(1 + \frac{X}{Y + N_0}\right)\right] = \int_0^{\infty} \frac{\mathcal{L}_Y(s) - \mathcal{L}_{X,Y}(s)}{s} \exp(-N_0 s) ds, \quad (31)$$

where $\mathcal{L}_Y(s)$ and $\mathcal{L}_{X,Y}(s)$ represent the LT of Y and joint LT of X and Y , respectively. Subsequently, we derive the ergodic capacity of the typical IRS-assisted user as follows:

$$R_{ID} = \int_0^{\infty} \frac{\mathcal{L}_{I_B}(s) \mathcal{L}_{I_R}(s) - \mathcal{L}_{I_B}(s) \mathcal{L}_{I_R}(s) \mathcal{L}_{S_{R_0}}(s)}{s} \exp(-N_0 s) ds, \quad (32)$$

Similarly, the ergodic capacity of the typical user in direct mode R_D is given as follows:

$$R_D = \int_0^\infty \frac{\mathcal{L}_{\hat{I}_B}(s)\mathcal{L}_{\hat{I}_R}(s) - \mathcal{L}_{\hat{I}_B}(s)\mathcal{L}_{\hat{I}_R}(s)\mathcal{L}_{S_{D_0}}(s)}{s} \exp(-N_0s) ds, \quad (33)$$

where $\mathcal{L}_{S_{D_0}}(s) = \mathbb{E}[\mathcal{L}_{S_{D_0}|d_0}(s)]$ and $\mathcal{L}_{S_{D_0}|d_0}(s) = \frac{1}{1+s\hat{P}\beta^2d_0^{-\alpha}}$.

D. Energy Efficiency

We define the energy-efficiency of a typical user by dividing the achievable rate with the network power consumption. The energy-efficiency of IRS-assisted user is given as follows:

$$EE_{ID} = \frac{\int_0^\infty \frac{\mathcal{L}_{I_B}(s)\mathcal{L}_{I_R}(s) - \mathcal{L}_{I_B}(s)\mathcal{L}_{I_R}(s)\mathcal{L}_{S_{R_0}}(s)}{s} \exp(-N_0s) ds}{p_{BS} + p_U + P + p_{IRS}}, \quad (34)$$

which is obtained by dividing (32) with p_{IRS} . Similarly, the energy-efficiency of a typical user in the direct communication mode EE_D can be given by dividing (33) with the power consumption in the direct mode \hat{P} as follows:

$$EE_D = \frac{\int_0^\infty \frac{\mathcal{L}_{\hat{I}_B}(s)\mathcal{L}_{\hat{I}_R}(s) - \mathcal{L}_{\hat{I}_B}(s)\mathcal{L}_{\hat{I}_R}(s)\mathcal{L}_{S_{R_0}}(s)}{s} \exp(-N_0s) ds}{p_{BS} + p_U + \hat{P}}. \quad (35)$$

E. Overall Network Coverage, Ergodic Capacity, and Energy Efficiency

The overall coverage probability of the typical user is derived as follows:

$$C = (1 - \mathcal{A})C_D + \mathcal{A}C_{ID}, \quad (36)$$

where \mathcal{A} represents the fraction of users in the system performing indirect IRS-assisted transmission, while $(1 - \mathcal{A})$ represents the fraction of users performing direct transmission. Similarly, the overall achievable rate and energy-efficiency of the typical user can be derived as follows: $R = (1 - \mathcal{A})R_D + \mathcal{A}R_{ID}$, and $EE = (1 - \mathcal{A})EE_D + \mathcal{A}EE_{ID}$, respectively.

The fraction of IRS-assisted and direct users can be perceived in many ways. For instance, it can be considered that the fraction of IRS-assisted users is proportional to the number of IRSs in the network. In this case, \mathcal{A} can be defined as $\frac{\lambda_R}{\lambda_R + \lambda_B}$. As an example, if there are five BSs and five IRSs, then $\mathcal{A} = 0.5$ assuming that one IRS can at-most provide service to one-user at a time. On the other hand, the fraction of IRS-assisted users can be considered proportional to the blocking probability of nearest direct link (as IRS is only associated to BS if there is a blocked direct link). For instance, considering a Boolean blockage model with the assumption that number of blockages follow Poisson distribution [34], the probability of direct transmission can be given as $\exp(-(\eta d_0 + u))$, where η and u are defined on the basis of the

shape of considered blockages [35]. Subsequently, the probability of blockages can be written as $\mathcal{A} = 1 - \exp(-(\eta d_0 + u))$. Considering blockage the SINR of the direct mode in (27) modifies as $\gamma_D = \mathcal{A} \frac{S_{D0}}{\hat{I}_B + \hat{I}_R + N_0}$ that results in modified coverage probability C_D in (28) as

$$C_D = \mathbb{E}_{d_0} \left[e^{-\frac{\tau d_0^\alpha N_0}{\mathcal{A} \beta^2 \hat{P}}} \mathcal{L}_{\hat{I}_B} \left(\frac{\tau d_0^\alpha}{\mathcal{A} \beta^2 \hat{P}} \right) \mathcal{L}_{\hat{I}_R} \left(\frac{\tau d_0^\alpha}{\mathcal{A} \beta^2 \hat{P}} \right) \right].$$

VI. NUMERICAL RESULTS AND DISCUSSION

In this section, we validate the accuracy of our derived expressions and then obtain useful insights related to different interference scenarios, the total number of IRSs in the setup, number of IRS elements and transmission power for different communication modes.

A. Simulation Parameters

Unless stated otherwise, the simulation parameters are listed herein. The heights of IRSs and BSs are set to $H_R = 10$ m, and $H_B = 20$ m, respectively. The coverage radius is $R = 700$ m. The transmission power for IRS-assisted mode and direct mode is $P = 20$ W and $\hat{P} = 20$ W, respectively. The static power consumption of BS and user is $p_{BS} = 40$ dBm and $p_U = 10$ dBm, respectively [36]. The phase resolution power consumption for 6- bits $p_r(6) = 78$ mW. The total number of IRS elements per IRS is $N = 50$, BS intensity within the coverage area is $\lambda_B = 10^{-4}$, and the total number of IRSs in the coverage area $M = 1500$ that corresponds to $\lambda_R = M/\pi R^2 \approx 10 \times \lambda_B$. Also, λ_R is IRS intensity, path-loss exponent is $\alpha = 4$, threshold on SINR $\tau = -10$ dB, and noise power spectral density is $N_0 = 10^{-10}$ W/Hz.

B. Validation of Analysis

Fig. 7 compares the coverage probability of IRS-assisted user and the user supported by the direct transmission as a function of the SINR threshold τ considering $P = \hat{P} = 20$ W. Numerical results show that our theoretical analysis and Monte-Carlo simulations match well. As expected, the conditional coverage probability decreases with the increase in SINR threshold for both types of users. Nevertheless, the coverage probability of IRS-assisted transmission lags behind the direct transmission even when the intensity of IRSs is higher than the intensity of BSs, i.e., $\lambda_R = 10\lambda_B$. This fact signifies the efficacy of IRS deployments mostly in scenarios when the direct transmission link is blocked.

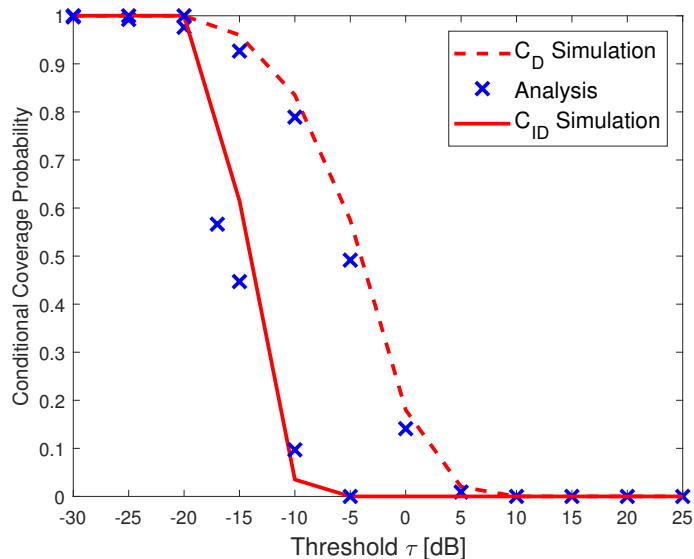


Fig. 7. Validation of conditional coverage probability in IRS-assisted and direct mode of communications derived in (23) and (28), using Monte-Carlo simulations.

C. Impact of BS Transmit Power on Direct Communication

Fig. 8 compares the achievable data rate of IRS-assisted communication and the direct mode considering $\hat{P} = 1$ W and $\hat{P} = 5$ W. We observe that for smaller number of IRS elements, direct transmissions outperform the IRS-assisted transmissions. As the number of IRS elements increases, R_{ID} increases because the IRS link gets stronger with more elements. An increase in IRS interference however degrades the achievable data rate R_D in direct links. The figure also depicts that the performance of IRS-assisted communication starts to exceed direct communication with lower IRS elements if the transmit power of BSs is low as can be seen from switching point $N = 30$ and $N = 60$ for $\hat{P} = 1$ and $\hat{P} = 5$, respectively. We note that, for a given deployment density of BSs and IRSs, IRS-assisted mode is useful for a larger number of IRS elements and low transmit power of BSs in direct mode. Evidently, a higher transmission power of direct user's BSs degrades IRS-assisted communication, which is opposite for direct communication.

Similarly, Fig. 9 validates the accuracy of energy-efficiency considering $\hat{P} = 1$ W and $\hat{P} = 5$ W. As expected, the IRS-assisted mode outperforms the direct mode for $N = 40$ and $N = 100$, for $\hat{P} = 1$ W and $\hat{P} = 5$ W, respectively. Compared to $\hat{P} = 5$ W, energy-efficiency is lower for $\hat{P} = 1$ W.

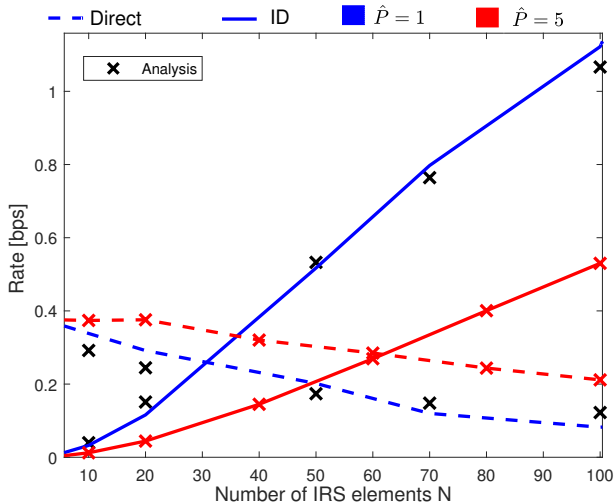


Fig. 8. Analytical and simulation results on conditional achievable rate in IRS-assisted and direct mode of communications derived in (32) and (33) with respect to IRS elements (for $\hat{P} = 1$ and $\hat{P} = 5$).

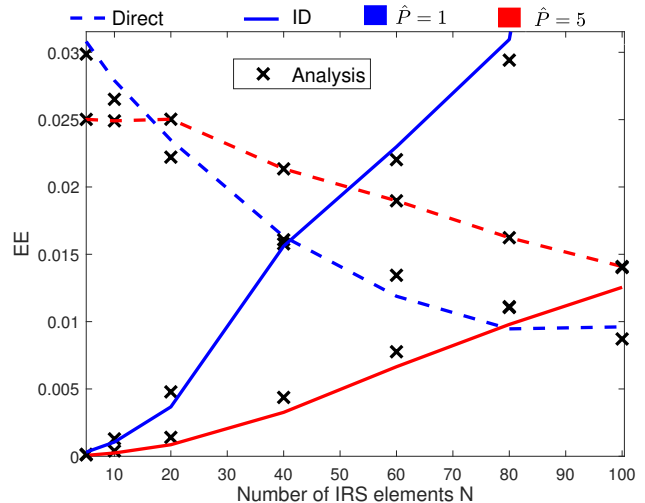


Fig. 9. Validation of conditional EE for IRS-assisted and direct mode of communications derived in (34) and (35), using Monte-Carlo simulations (for different number of IRS elements, $\hat{P} = 1$ and $\hat{P} = 5$).

D. Impact of IRS Intensity on Direct and IRS-Assisted Communications

Fig. 10 compares the coverage probability and rate for direct and IRS-assisted communication as a function of the total number of IRS elements and IRSs within the cell radius. We note that varying the number of IRS elements per IRS have no significant impact on the coverage probability and rate for sparse deployment of IRSs $M = 300$. However, the coverage probability C_{ID} and achievable rate R_{ID} increases with the increase in number of IRS elements for dense deployment of IRSs $M = 1500$. This is encouraging as it shows that the impact of interference due to dense deployment of IRSs is not significant. On the other hand, the rate of the direct communication decreases with the increasing IRS elements, especially for dense deployment of IRSs since the IRS interference becomes significantly dominant.

Fig. 11 shows power consumption and EE for the IRS-assisted and the direct modes of communication with respect to the number of IRSs $M = 300$ and $M = 1500$. The figure presents that the p_{ID} increases with the increase in N as expected since $p_{ID} \propto N$. However, the direct mode power consumption p_D remains same since p_D is not the function of N . It is also clear that M does not have any impact on the power consumption since p_{ID} is defined based on total system power consumption per user (refer to Section II-D) and a user is assumed to

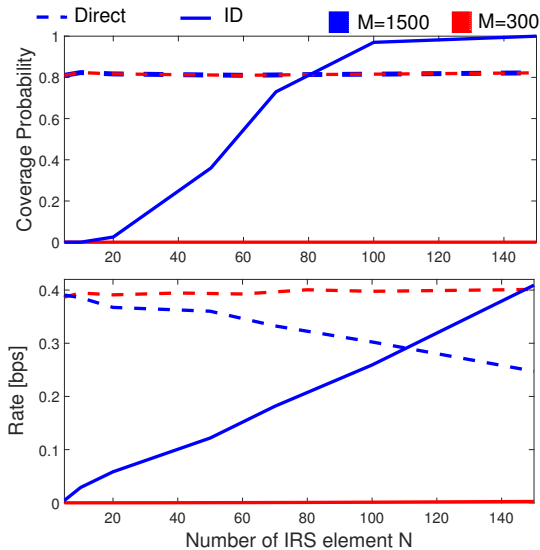


Fig. 10. Comparison of conditional coverage probability and achievable rate for IRS-assisted mode and direct mode of communications with respect to number of IRS elements (for total number of IRSs $M = 300$ and $M = 1500$).

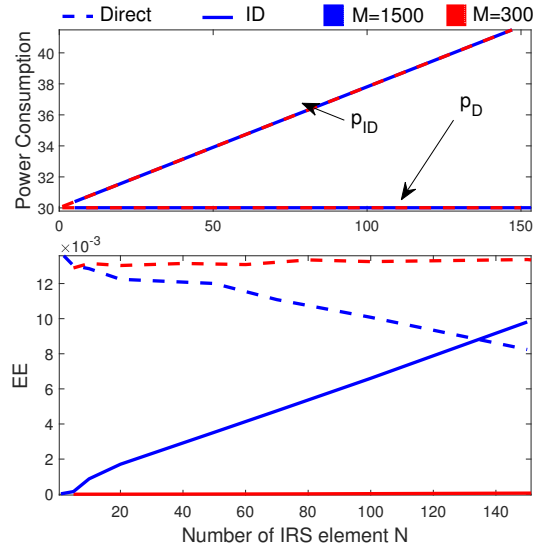


Fig. 11. Comparison of power consumption and conditional EE for IRS-assisted mode and direct mode of communications with respect to number of IRS elements (for total number of IRSs $M = 300$ and $M = 1500$).

be connected with only one IRS at a time. The energy efficiency follows the same trend as conditional rate yet with the smaller slope due to the increasing power of indirect mode that appears in the denominator of EE.

E. Impact of BS Intensity on Direct and IRS-Assisted Communications

Fig. 12 compares the coverage probability and ergodic capacity for IRS-assisted and direct communication with respect to total number of IRSs in the coverage area for BS intensity $\lambda_B = 10^{-4}$ and $\lambda_B = 0.5 \times 10^{-4}$. We observe that C_{ID} increases as total number of IRSs in the cell increases. Also, a very subtle decrease in C_D is observed for both $\lambda_B = 10^{-4}$ and $\lambda_B = 0.5 \times 10^{-4}$. This is because, as M increases, the IRS density increases and the nearest IRS becomes closer to the user that corresponds to smaller $r_{0,0}$ and higher IRS received signal power that leads to improvement in C_{ID} . Also, an increases in M increases the interference coming from the IRSs for the direct user resulting in a slight decrease in C_D . The figure also shows that a more sparse BS deployment leads to a smaller coverage probability of direct communication mode, and indirect coverage C_{ID} outperforms direct mode coverage for $M > 1700$ for both the values of λ_B . A similar trend can be observed for the achievable rate. This implies that density

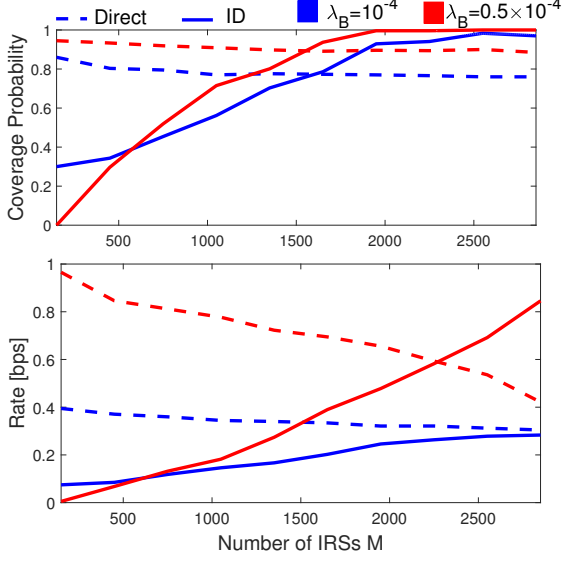


Fig. 12. Comparison of conditional coverage probability and achievable rate for IRS-assisted mode and direct mode of communications with respect to total number of IRSs (for BS intensity $\lambda_B = 10^{-4}$ and $\lambda_B = 0.5 \times 10^{-4}$, and $N = 100$).

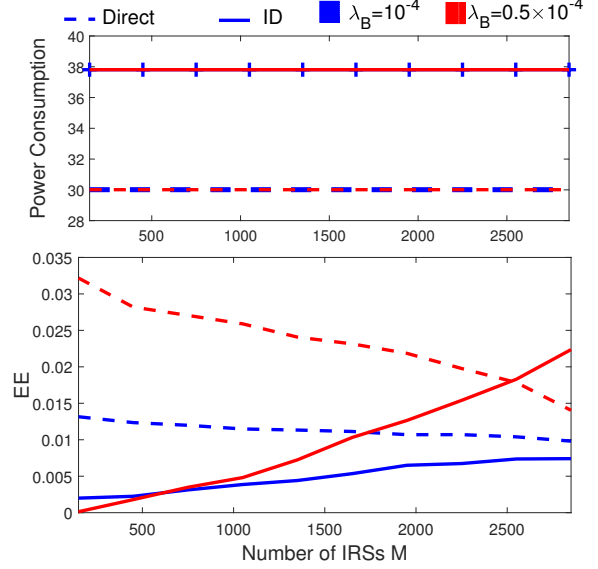


Fig. 13. Comparison of power consumption and conditional EE for IRS-assisted mode and direct mode with respect to total number of IRSs (for BS intensity $\lambda_B = 10^{-4}$ and $\lambda_B = 0.5 \times 10^{-4}$, and $N = 100$).

of deployment of IRSs (i.e., sparse BS deployment or dense IRS deployment) plays a significant role in the performance of IRS-assisted mode.

Fig. 13 presents results on power consumption and EE for the direct and indirect modes. Fig. 13 follows the same trend of achievable rate as in Fig. 12 with the difference in the slope of EE_{ID} .

Fig. 14 shows the impact of \mathcal{A} on different system performance measures. The coverage probability of IRS-assisted communication C_{ID} increases with \mathcal{A} because this increases $\lambda_R = \frac{\mathcal{A}}{1-\mathcal{A}}\lambda_B$. The overall system coverage probability P_C follows C_D when $\mathcal{A} \approx 0$ which corresponds to very few or no IRS in the system. However, P_C decreases up to $\mathcal{A} = 0.6$ and then it starts to increase and converges to C_{ID} when $\mathcal{A} \approx 1$ for $N = 100$. Note that, for $\mathcal{A} \approx 0.95$, $\lambda_R = 20\lambda_B$. Moreover, a decrease in direct coverage probability C_D is also visible due to the aggregate interference coming from IRS. A similar trend is observed for $N = 50$ with poorer C_{ID} than C_D due to fewer IRS elements compared to the case when $N = 100$. Also, Fig. 15 shows a similar trend in achievable rate because the power consumption does not change significantly.

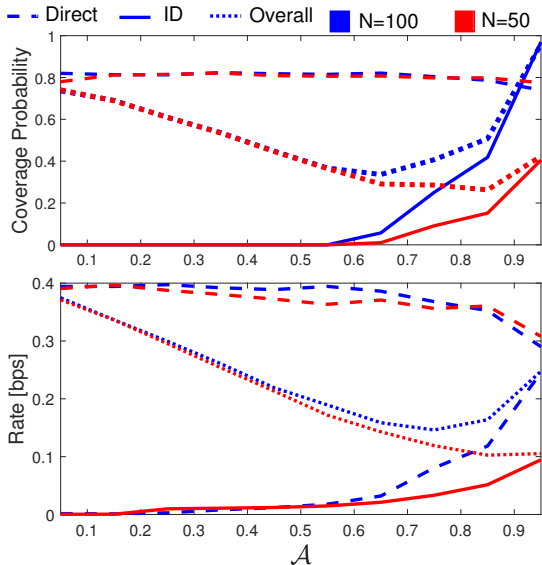


Fig. 14. Comparison of conditional coverage probability and achievable rate for IRS-assisted mode and direct mode, and overall performance with respect to the fraction of users assisted by IRS \mathcal{A} (for number of IRS elements $N = 50$ and $N = 100$ per IRS surface).

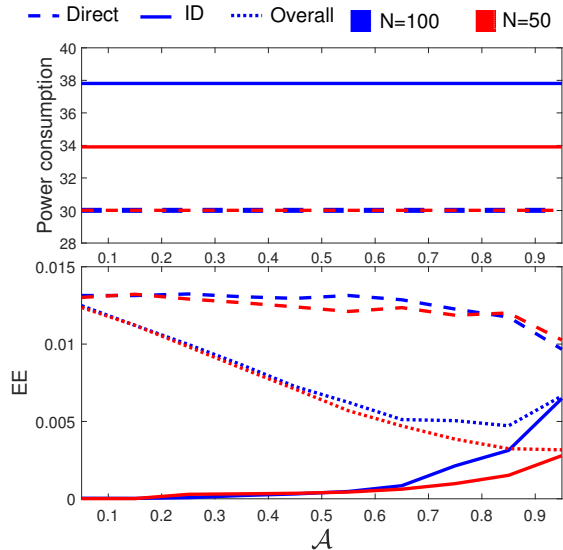


Fig. 15. Comparison of power consumption, conditional energy-efficiency for IRS-assisted mode, direct mode, and overall EE with respect to the fraction of users assisted by IRS \mathcal{A} (for number of IRS elements $N = 50$ and $N = 100$ per surface).

VII. CONCLUSION

We have analyzed the downlink coverage probability, ergodic capacity, and energy-efficiency performance for cellular networks under multi-BS and multi-IRS setup considering both the IRS-assisted communication and direct communication modes. We have observed that using a larger number of IRS elements per IRS are crucial for IRS-assisted communication to outperform direct communication. Also, we have observed that IRS-assisted communication becomes dominant when IRSs are densely deployed (i.e., when IRS intensity is larger than BS intensity). Also, for dense IRS deployment, the impact of IRS-interference significantly decreases the performance of direct communication and enhances IRS-assisted communication because the nearest IRS becomes closer to user. Our results also have demonstrated the impact of fraction of indirect IRS-assisted users on the overall system performance and given insights on how to select the proportion of direct or indirect IRS-assisted users in the network to achieve the desired trade-off between the degradation of direct communication and massive connectivity. The work can be extended to investigate the impact of multi-antennas at the BSs and the user devices.

REFERENCES

- [1] Q. Wu and R. Zhang, "Towards smart and reconfigurable environment: Intelligent reflecting surface aided wireless network," *IEEE Commun. Mag.*, vol. 58, no. 1, pp. 106–112, 2020.
- [2] Q. Wu, S. Zhang, B. Zheng, C. You, and R. Zhang, "Intelligent reflecting surface aided wireless communications: A tutorial," *IEEE Trans. Commun.*, 2021.
- [3] C. Huang, A. Zappone, G. C. Alexandropoulos, M. Debbah, and C. Yuen, "Reconfigurable intelligent surfaces for energy efficiency in wireless communication," *IEEE Trans. Commun.*, vol. 18, no. 8, pp. 4157–4170, 2019.
- [4] C. Liaskos, S. Nie, A. Tsioliaridou, A. Pitsillides, S. Ioannidis, and I. Akyildiz, "A new wireless communication paradigm through software-controlled metasurfaces," *IEEE Commun. Mag.*, vol. 56, no. 9, pp. 162–169, 2018.
- [5] E. Basar, M. Di Renzo, J. De Rosny, M. Debbah, M.-S. Alouini, and R. Zhang, "Wireless communications through reconfigurable intelligent surfaces," *IEEE Access*, vol. 7, pp. 116 753–116 773, 2019.
- [6] D. Kudathanthirige, D. Gunasinghe, and G. Amarasinghe, "Performance analysis of intelligent reflective surfaces for wireless communication," in *IEEE Intl. Conf on Commun. (ICC)*, 2020, pp. 1–6.
- [7] L. Yang, F. Meng, Q. Wu, D. B. da Costa, and M.-S. Alouini, "Accurate closed-form approximations to channel distributions of RIS-aided wireless systems," *IEEE Wireless Commun. Letters*, vol. 9, no. 11, pp. 1985–1989, 2020.
- [8] A.-A. A. Boulogeorgos and A. Alexiou, "Performance analysis of reconfigurable intelligent surface-assisted wireless systems and comparison with relaying," *IEEE Access*, vol. 8, pp. 94 463–94 483, 2020.
- [9] I. Trigui, W. Ajib, and W.-P. Zhu, "A comprehensive study of reconfigurable intelligent surfaces in generalized fading," *arXiv preprint arXiv:2004.02922*, 2020.
- [10] H. Ibrahim, H. Tabassum, and U. T. Nguyen, "Exact coverage analysis of intelligent reflecting surfaces with Nakagami-m channels," *IEEE Trans. Vehicular Technol.*, vol. 70, no. 1, pp. 1072–1076, 2021.
- [11] Q. Tao, J. Wang, and C. Zhong, "Performance analysis of intelligent reflecting surface aided communication systems," *IEEE Commun. Letters*, vol. 24, no. 11, pp. 2464–2468, 2020.
- [12] T. Van Chien, A. K. Papazafeiropoulos, L. T. Tu, R. Chopra, S. Chatzinotas, and B. Ottersten, "Outage probability analysis of IRS-assisted systems under spatially correlated channels," *IEEE Wireless Commun. Letters*, 2021.
- [13] Z. Peng, T. Li, C. Pan, H. Ren, W. Xu, and M. Di Renzo, "Analysis and optimization for RIS-aided multi-pair communications relying on statistical CSI," *IEEE Trans. Vehicular Technol.*, 2021.
- [14] L. Yang, Y. Yang, D. B. da Costa, and I. Trigui, "Outage probability and capacity scaling law of multiple RIS-aided networks," *IEEE Wireless Commun. Letters*, 2020.
- [15] D. L. Galappaththige, D. Kudathanthirige, and G. A. A. Baduge, "Performance analysis of distributed intelligent reflective surface aided communications," in *IEEE Global Commun. Conf. (GLOBECOM)*, 2020, pp. 1–6.
- [16] T. N. Do, G. Kaddoum, T. L. Nguyen, D. B. da Costa, and Z. J. Haas, "Multi-RIS-aided wireless systems: Statistical characterization and performance analysis," *arXiv preprint arXiv:2104.01912*, 2021.
- [17] Y. Zhu, G. Zheng, and K.-K. Wong, "Stochastic geometry analysis of large intelligent surface-assisted millimeter wave networks," *IEEE J. Select Area. Commun.*, vol. 38, no. 8, pp. 1749–1762, 2020.
- [18] J. Lyu and R. Zhang, "Hybrid active/passive wireless network aided by intelligent reflecting surface: System modeling and performance analysis," *arXiv preprint arXiv:2004.13318*, 2020.
- [19] E. Björnson and L. Sanguinetti, "Power scaling laws and near-field behaviors of massive MIMO and intelligent reflecting surfaces," *arXiv preprint arXiv:2002.04960*, 2020.
- [20] C. Huang, G. C. Alexandropoulos, A. Zappone, M. Debbah, and C. Yuen, "Energy efficient multi-user MISO communication using low resolution large intelligent surfaces," in *IEEE Globecom Workshops (GC Wkshps)*, 2018, pp. 1–6.

- [21] K. A. Hamdi, "A useful lemma for capacity analysis of fading interference channels," *IEEE Trans. Commun.*, vol. 58, no. 2, pp. 411–416, 2010.
- [22] J. Salo, H. M. El-Sallabi, and P. Vainikainen, "The distribution of the product of independent Rayleigh random variables," *IEEE Trans. Antennas Propag.*, vol. 54, no. 2, pp. 639–643, 2006.
- [23] H. Lu, Y. Chen, and N. Cao, "Accurate approximation to the pdf of the product of independent rayleigh random variables," *IEEE Antennas Wireless Propag. Letters*, vol. 10, pp. 1019–1022, 2011.
- [24] E. W. Stacy *et al.*, "A generalization of the gamma distribution," *The Annals of mathematical statistics*, vol. 33, no. 3, pp. 1187–1192, 1962.
- [25] A. Jeffrey and D. Zwillinger, *Table of integrals, series, and products*. Elsevier, 2007.
- [26] S. P. Boyd and L. Vandenberghe, *Convex Optimization*. Cambridge University Press, 2004.
- [27] Q. Wu and R. Zhang, "Intelligent reflecting surface enhanced wireless network via joint active and passive beamforming," *IEEE Trans. Commun.*, vol. 18, no. 11, pp. 5394–5409, 2019.
- [28] "NIST Digital Library of Mathematical Functions," <http://dlmf.nist.gov/>, Release 1.1.1 of 2021-03-15, f. W. J. Olver, A. B. Olde Daalhuis, D. W. Lozier, B. I. Schneider, R. F. Boisvert, C. W. Clark, B. R. Miller, B. V. Saunders, H. S. Cohl, and M. A. McClain, eds. [Online]. Available: <http://dlmf.nist.gov/>
- [29] T. Shafique, H. Tabassum, and E. Hossain, "Optimization of wireless relaying with flexible UAV-borne reflecting surfaces," *IEEE Trans. Commun.*, vol. 69, no. 1, pp. 309 – 325, 2021.
- [30] M. A. Kishk and M.-S. Alouini, "Exploiting randomly-located blockages for large-scale deployment of intelligent surfaces," *arXiv preprint arXiv:2001.10766*, 2020.
- [31] M. Di Renzo and P. Guan, "Stochastic geometry modeling of coverage and rate of cellular networks using the Gil-Pelaez inversion theorem," *IEEE Commun. Letters*, vol. 18, no. 9, pp. 1575–1578, 2014.
- [32] S. Srinivasa and M. Haenggi, "Distance distributions in finite uniformly random networks: Theory and applications," *IEEE Trans. Vehicular Technol.*, vol. 59, no. 2, pp. 940–949, 2009.
- [33] H. Tabassum and E. Hossain, "Coverage and rate analysis for co-existing RF/VLC downlink cellular networks," *IEEE Trans. Commun.*, vol. 17, no. 4, pp. 2588–2601, 2018.
- [34] J. Sayehvand and H. Tabassum, "Interference and coverage analysis in coexisting RF and dense Terahertz wireless networks," *IEEE Wireless Commun. Letters*, vol. 9, no. 10, pp. 1738–1742, 2020.
- [35] T. Bai, R. Vaze, and R. W. Heath, "Analysis of blockage effects on urban cellular networks," *IEEE Trans. Wireless Commun.*, vol. 13, no. 9, pp. 5070–5083, 2014.
- [36] M. Zhang, L. Tan, K. Huang, and L. You, "On the trade-off between energy efficiency and spectral efficiency in RIS-aided multi-user MISO downlink," *Electronics*, vol. 10, no. 11, p. 1307, 2021.